Early Th2 cytokine production in *Heligmosomoides polygyrus* and *Toxoplasma gondii* co-infected mice is associated with reduced IFNγ production, increased parasite loads and increased mortality

Edina K. Szabo[1], Christina Bowhay[1], Namratha Badawadagi[1], Beatrice Fung[1], Camila Gaio[1], Kayla Bailey[1], Manfred Ritz[1], Anupama Ariyaratne[1], Joel Bowron[1] & Constance A. M. Finney[1*]

[1]Department of Biological Sciences, Faculty of Science, University of Calgary, Calgary, Alberta, Canada.

Corresponding Authors: Constance A. M. Finney, constance.finney@ucalgary.ca, Faculty of Science, Department of Biological Sciences, University of Calgary, 2500 University Drive N.W., Calgary, Alberta, Canada.

Running Title: Impact of parasite co-infection on host immunity

Keywords: Nematodes, Helminth, Co-infection, Toxoplasma, Innate Immunity, Adaptive Immunity, IFNγ, Th2 cytokines

ABSTRACT

Co-infections are a common reality but understanding how the immune system responds in this context is complex and can be unpredictable. Despite this, it is key to develop models that will provide better translatability to real world situations. *Heligmosomoides polygyrus* (parasitic roundworm) and *Toxoplasma gondii* (protozoan parasite) are well studied organisms that stimulate a characteristic Th2 and Th1 response respectively. IFNγ-producing T cells, NK and γδ T cells contribute to early protective immunity during *T. gondii* infection. To minimise immunopathology, IL-10 is also key to a successful response. Previous research has found *H. polygyrus* to improve survival during co-infection with both parasites. IFNγ-producing $CD4^+$ and $CD8^+$ T cells were implicated in this protection. Using a similar approach, we have found the opposite. Our co-infected animals displayed greater mortality and intestinal pathology than either single infection. This was associated with an early increase in Th2 cytokines in the Peyer's patches, mesenteric lymph nodes and spleen. Co-infected animals also had reduced IFNγ–producing cells at day 5 post *T. gondii* infection in the Peyer's patches (CD8 T cells only) and in the MLN (NK, NKT, γδ T, $CD4^+$ T and $CD8^+$ T cells). This correlated with increased parasite loads in the MLN at 10 days post *T. gondii* infection. Our results demonstrate that co-infection dynamics can vary dramatically and that careful consideration needs to be taken when interpreting data in each situation.

INTRODUCTION

Co-infections are a common reality [1]. However, understanding the complexities which underlie their impact on host immune responses remains difficult. Data are conflicting and impacted by a number of variables which include host and parasite genetics, age, immune history and nutrition to name but a few. Despite this, there is a need to unpick the simplified scenarios that can be set up in a laboratory and apply them to the real world.

Co-infection by pathogens stimulating different arms of the immune response can result in a number of different outcomes [2] although certain traits are thought to predict the interplay between multiple infectious agents. For example, parasite infection dynamics can be predicted by the type of immune effector mechanisms required to clear infection, as well as the ability of parasites to induce immunosuppression [3]. Both these traits are defined by specific cytokine signatures. Changes in the characteristic signatures can have significant impacts on disease management. This is particularly important in the context of parasitic worm infections since intestinal roundworm infections are so common in humans (approximately 1.8 billion infections worldwide [4], livestock [5] and wildlife [6]. These parasites negatively impact vaccine and treatment efficacy [3],[7], which can be restored with anthelminthic treatment that clear the worms [8].

The intestinal mucosa is continually subjected to a multitude of pathogens and commensals. The interplay between these different players impacts the ability of the immune system to

maintain a strong barrier and contain these populations. The gut-associated lymphoid tissue (GALT), including the mesenteric lymph nodes (MLN), Peyer's Patches (PP) and the small intestine (SI), represents the largest lymphatic mass in the body. Trafficking to and interactions between lymphocytes in these sites are important in host defence. Through interactions between the intestine and the GALT/MLN, homing of activated lymphocytes to the gut mucosa is achieved during intestinal inflammation [9]. Here, we used two parasites that stimulate opposing immune responses in the small intestine and the GALT.

Heligmosomoides polygyrus (Hp) is a parasitic nematode (roundworm) which matures within the intestinal tissue and causes a chronic infection whereby adult worms reproduce and lay eggs in the intestinal lumen [10]. The immune response to this parasite has been well characterised. To clear worms, the host stimulates a potent Th2 immune response leading to the formation of a Th2 granuloma that allows the trapping/killing of larvae. Antibodies and intestinal physiological responses also promote worm killing/expulsion. In conjunction, a Treg response is mounted, thought to limit any potentially immunopathological Th1 response [11]. However, in susceptible mice (C57Bl/6 mice, used here), the granulomas and Th2 response are not strong enough to clear the worms [12] and the infection remains chronic.

Toxoplasma gondii (Tg) is an intracellular parasite that first infects intestinal cells, followed by multiple other cell types as it spreads systemically [13]. The host response to Tg is a strong inflammatory response involving IFNγ production by lymphocytes. NK cells are essential for the early control of Tg [14]–[16], as is the induction of $CD8^+$ T cells [17]. Similarly, Tg infection

studies demonstrate that γδ T depleted mice are less resistant to Tg than their wildtype counterparts, due to the early IFNγ production of γδ T cells during infection [18],[19]. The role of NKT cells however is not clear during *T. gondii* infection. While they play a large part in the induction and initiation of inflammatory responses, this can lead to overproduction of IFNγ, which can be detrimental for the host [20]. Others have found that NKT cells may even be directly involved in the suppression of protective immunity against Tg [21]. However, most studies published on helminth-Tg co-infections focus on IFNγ production by conventional T cells (CD4+ and CD8+ T cell) [22]–[24] with much less known about the role of other lymphocyte populations (e.g. γδ T and NKT cells). Finally, as well as a strong IFNγ response, Tg stimulates high levels of IL-10 to limit immunopathology [25].

Several studies have demonstrated reduced inflammatory cytokine responses in animals co-infected with an intestinal nematode and a microparasite such as Tg [23],[24],[26],[27]. However, while general cytokine signatures have been examined, the impact on the different cytokine producing lymphocytes is not fully understood. To shed more light on the lymphocyte response in the context of HpTg co-infection, we investigated the changes of Th1 and Th2 cytokines, as well as the IFNγ-producing lymphocytes (NK, NKT, $CD4^+$ T, $CD8^+$ T and γδ T cells) at day 5 and day 10 post-Tg infection in a number of different organs. Most studies have focused on organs that are distant to the infection site (e.g. spleen (SPL), Liver (LIV) and MLN). Few studies like us have also focused on the SI, which is Hp's niche and is Tg's first contact with the host, or on the PP which are intricately linked to the SI. This is important since lymphocytes generally display distinct phenotypes and functions in different organs [28].

We detected early increases in Th2 cytokines in the PP, MLN and SPL of HpTg animals. Co-infected animals also had reduced IFNγ–producing cells at day 5 post Tg infection in the PP ($CD8^+$ T cells only) and in the MLN (all lymnphocytes: NK, NKT, γδ T, $CD4^+$ T and $CD8^+$ T cells). This correlated with increased Tg loads in the MLN at 10 days post Tg, increased Hp loads, increased intestinal pathology and reduced survival compared to Tg animals.

METHODS

Animals, Parasites and Infection Protocols

C57BL/6 female mice, aged between 8-10 weeks old, were bred in house at the University of Calgary. Breeding pairs were originally purchased from Charles River Laboratories (Senneville, Quebec). All mice were housed under specific pathogen-free conditions. The University of Calgary's Animal Care Committee approved all experimental animal procedures.

The Me49 strain of *Toxoplasma gondii* (Tg) (maintained in house, original stock was a gift from Dr. Georgia Perona Wright, University of British Columbia, Canada) was maintained in male C57BL/6 mice by bimonthly passage into new animals. Cysts were obtained from the brains of these animals a month after infection. Brains of infected mice were homogenised in PBS to count tissue cysts. 20 cysts were orally administered per mouse (female C57BL/6). Animals were euthanized either 5 or 10 days post infection.

Female C57BL/6 mice were infected with 200 *Heligmosomoides polygyrus* (Hp) infective larvae (maintained in house, original stock was a gift from Dr. Allen Shostak, University of Alberta, Canada). Animals were euthanized either 12 or 17 days post infection. Larvae were obtained from fecal cultures after approximately 8-9 days of incubation at room temperature.

For co-infected animals, mice were first infected with *Hp* for 7 days. At day 7 post-infection, animals were orally infected with 20 cysts of the Me49 strain of *Tg* (all other experimental animals were gavaged with PBS as a control). Mice were euthanized 5 or 10 days post *Tg* infection (equivalent to 12 or 17 days post *Hp* infection).

For worm counts, small intestines of Hp and HpTg infected mice were harvested and opened longitudinally. The number of adult worms present in the intestinal lumen along the length of the small intestine was counted under a dissection microscope.

Histopathology

Small intestines, spleens and livers were isolated and fixed in 4% paraformaldehyde. Paraffin embedded sections were obtained for each tissue and stained with hematoxylin and eosin (H&E) and/or hematoxylin and alcian blue (for goblet cell counts in the small intestine). Stained tissue sections were analysed visually using the Leica DMRB light microscope and/or the OLMYPUS SZX10 microscope according to a scoring system developed by the Finney group (Sup. Fig. 1 & 2, and Sup. Tables 1-3). Images were captured using the QCapture and the cellSens software and processed using the ImageJ software.

For the spleen and liver scoring systems, slides were blindly evaluated by two independent researchers at x40 magnification. Three scoring parameters were developed for the spleen: follicle shape, marginal zone thickness and size of the germinal center (light zone). For the liver,

we used the presence/absence of necrosis, infiltrate size, proportion of infiltrates, perivascular infiltrate characteristics. The parameters within each scheme were given an equal weighting and were combined to give a total, gross pathological score for each slide. A higher score is representative of a greater amount of observed tissue damage.

For goblet cell counts, the average number of goblet cells from five consecutive villi was calculated for each animal in the proximal and distal SI. The villi perimeters were calculated using ImageJ.

Serum ELISAs

Blood samples were collected using a terminal cardiac bleed. Blood was left to clot for 30 minutes and then centrifuged twice at 11, 000 g at 4^{o}C for 10 minutes.

IFNγ cytokine production was measured in the serum of Tg and HpTg infected, and naive mice with the Mouse DuoSet ELISA development system (R&D Systems), according to the manufacturers' instructions.

RNA/DNA Extraction and Quantitative PCR

RNA and gDNA was extracted from snap frozen SPL, LIV, MLN, PP, and 4 equal sections of the SI (sections 1-4, where 1 is the most proximal section and 4 the most distal) by crushing the tissue

using a pestle and mortar on dry ice and using Trizol (Ambion, Life Technologies) following manufacturer guidelines.

To measure cytokine levels in the RNA samples, cDNA was prepared using Perfecta DNase I (Quanta), and qScript cDNA Supermix (Quanta) or iScript Reverse Transcription Supermix for RT-qPCR (Bio-Rad).

Primers for quantitative PCR were obtained from Integrated DNA Technologies (San Diego). For IFNγ TCAAGTGGCATAGATGTGGAAGAA forward, and TGGCTCTGCAGGATTTTCATG reverse, IL-10 GTCATCGATTTCTCCCCTGTG forward, and ATGGGCCTTGTAGACACCTTG reverse, IL-4 CGAAGAACACCACAGAGAGTGAGCT forward, and GACTCATTCATGGTGCAGCTTATC reverse, IL-13 GATCTGTGTCTCTCCCTCTGA forward, and GTCCACACTCCATACCATGC reverse, and β-actin GACTCATCGACTCCTGCTTG forward, and GATTACTGCTCTGGCTCCTAG reverse primers were used. To confirm primer product size, all products were run on a gel. Samples were run on a Bio-Rad CFX96 real time system C1000 touch thermocycler. Relative quantification of the cytokine genes of interest was measured with the delta-delta cycle threshold quantification method [29], with β-actin for normalization. Data are expressed as a fold change relative to uninfected samples.

To quantify the *T. gondii* parasite burdens in the gDNA samples, we used a standard curve of *T. gondii* tachyzoites. *T. gondii* B1 was the target gene for the quantification of parasite in all tissues

or organs [30]. B1 primers (Forward: TCCCCTCTGCTGGCGAAA, reverse: AGCGTTCGTGGTCAACTATCGATT) were prepared by IDT (San Diego).

Flow Cytometry

Cell suspensions were obtained from the MLN, and LIV. For the MLN, cells suspensions were obtained through mechanical disruption of whole tissues. Perfused liver lobes were homogenised as per MLN. Lymphocytes were isolated from the cell suspension using a 37 % and 70 % percoll gradient (GE Healthcare Bio-Sciences AB, Sweden) diluted with HBSS (with or without phenol red, Lonza, Switzerland), and resuspended in RPMI.

For *ex vivo* restimulation, cells were incubated with 50ng/mL phorbol myristate acetate and 1 µg/mL ionomycin for 6 h at 37 °C with 5% CO_2 in the presence of BD GolgiStop. Single cell suspensions for all tissue types were stained and analysed according to [31]. Cells were in stained for: viability (APC-H7 or AF700, BD Biosciences), surface markers: CD45 (BV510), CD3 (BV605), CD4 (PerCP-Cy5.5), CD8 (BUV395), NK1.1 (BV421), γδ TCR (BV711) and intracellular markers: IFNγ (APC), and granzyme B (FITC). All antibodies were purchased from BD Biosciences apart from CD4 (PerCP-Cy5.5, BioLegend), Granzyme B (FITC, eBioscience). Cells were blocked with rat α-mouse CD16/32 (Biolegend). Cells were run on an LSRFortessa X-20 flow cytometer and data analysed using FlowJo software. For analysis, doublets and dead cells were removed from the analysis, and NK, NKT, γδ T, CD4 T and CD8 T IFNγ and GrzmB producing cells were quantified (Sup. Fig 3).

Statistical Analysis

GraphPad Prism software (La Jolla, CA, USA) was used for all statistical analysis. To compare multiple groups (three or more), we performed a normality test (Anderson-Darling normality test). ANOVA or Kruskal-Wallis tests were performed on parametric/non-parametric pooled data, and when significant, Sidak's/Dunn's Multiple comparisons were performed on Hp vs. HpTg and Tg vs. HpTg. For survival analysis, we used a Mantel-Cox test. Data are presented as median and individual data points, unless otherwise specified.

RESULTS

Increased mortality of HpTg infected mice correlates with increased intestinal, but not spleen or liver, pathology.

200 *H. polygyrus* larvae (L3) were orally administered to female C57Bl/6 mice 7 days prior to infection with 20 Me49 *T. gondii* tissue cysts. Animals infected with both parasites (HpTg) died earlier than mice with *T. gondii* infection alone (Tg), while all mice survived with single *H. polygyrus* (Hp) infection (Fig. 1A). Over 60% of Tg infected mice survived, but fewer than 20% of HpTg animals survived until day 16.

Tg and Hp both infect their host via the small intestine. Hp has an entirely enteric lifecycle, with larval stages developing within the intestinal tissue and adult stages residing in the intestinal lumen [32]. In contrast, Tg first invades the lamina propria of the small intestine, then disseminates throughout the body as early as day 3 post-infection [13],[33],[34]. Increased Tg burden has been associated with more severe pathology and death [35]. Therefore, we next investigated whether the increased mortality rate observed in co-infected animals correlated with increased intestinal pathology. Whole small intestines were formalin fixed, paraffin embedded and stained with either hematoxylin and eosin to investigate intestinal pathology or Alcian blue and hematoxylin to investigate goblet cell numbers. Goblet cells serve an important physical barrier against pathogens through the maintenance and production of mucus layer in the small intestine by the production of mucins [36]. Our data show significant differences in

pathology of the small intestine between Tg and HpTg infected animals (Fig. 1B). HpTg infected mice had pathology resulting from both Hp (granulomas) and Tg (inflammatory infiltrates) parasites (described in Sup. Table 1). However, the decrease in villi perimeter and goblet cell number observed in the proximal small intestine of Tg infected mice at d5 (day 5) post-infection was not observed in HpTg animals (Fig. 1B). No differences between any of the groups was observed in the villi perimeter length and goblet cell number at d10 post-infection in the proximal small intestine, or in the distal small intestine at either d5 or d10 post-infection (data not shown).

After having replicated in the intestinal tissue, Tg rapidly disseminates to other organs, including the spleen and liver. Analysis of spleen and liver sections indicate that Tg and HpTg infected animals had similar severe pathologies, while Hp infected animals were far less affected (Fig. 1. C&D, Sup. Table 2 & 3, Sup. Fig. 1 & 2). At d5 post-infection, spleens from all three infected groups looked similar with distinct follicles and marginal zones (mean pathology score of 5.3). However, by day 10, in both Tg and HpTg animals, the follicles and marginal zones had completely disappeared resulting in a highly disorganised structure (mean pathology score of 9.5). At day 5 in the liver, mild pathology was observed in Tg and HpTg infected groups characterised by small leukocyte infiltrates (mean pathology score of 7.8, +/- 0.2 SD, and 9.7,+/- 0.9 SD) compared to Hp infected animals (mean pathology score of 6.9, +/- 2 SD, respectively). By day 10, the pathology was much more severe with larger leukocyte infiltrates and areas of necrosis observed (mean pathology score of 12.3, +/- 1.4 SD for the Tg group, and 14.4, +/- 2.4 SD for the HpTg group, Fig 1D).

Commonly Me49 infection culminates in brain tissue being invaded by approximately 3 weeks post-infection. No tissue cysts were found in any of the infected mice at d5 or day 10 post-infection, or at the time of death (up to day 16 post-infection).

Parasite burdens of HpTg co-infected animals are increased compared to single infections.

Based on the pathology results, we hypothesized that not only the presence of both Hp and Tg, but also the increase in parasite burden was contributing to the reduced survival of the HpTg infected animals. Hp burden was measured by manually counting adult parasites in the intestinal lumen. Adult worm numbers were increased in HpTg compared to Hp infected mice at d5 and d10 post Tg infection (Fig. 2A). Tg burden was measured in all organs (SI, PP, MLN, SPL and LIV) using qRT-PCR, quantified to a known standard of parasites. In all organs, parasite loads increased from day 5 to day 10 post-infection (Fig 2B-F). The highest levels were observed in the lymphoid organs: PP (approximate mean of 1x10^8 parasites at d10 post-infection, Fig 2C), followed by the MLN (approximate mean of 1x10^7 parasites at d10 post-infection, Fig 2D) and SPL (approximate mean of 0.9x10^8 parasites at d10 post-infection, Fig 2E). In all organs/time points studied Tg burden did not differ between Tg and HpTg infected mice, with one notable exception: Tg levels were increased in the MLN of HpTg compared to Tg infected mice at d10 post infection, with an average of 9.8x10^7 (+/- 3.2 S.D) parasites in HpTg animals and only 2.0x10^7 (+/- 4.4 S.D) parasites in Tg animals (Fig 2B-F).

IFNγ gene expression in HpTg mice mirrors that of Tg infected mice, except in the MLN at day 5 post-infection.

Th1 responses, specifically IFNγ produced by NK and $CD8^+$ T cells, are crucial for protection against Tg [14],[37]–[42]. A lack of sufficient IFNγ production early during infection results in increased replication of Tg [43],[44]. To assess whether the increased Tg parasite loads observed in HpTg mice were associated with decreased IFNγ production, we measured IFNγ protein levels in the serum and gene expression levels in the SI, PP, MLN, SPL and LIV. Our data show increased levels of IFNγ in all samples tested for the Tg and HpTg groups compared to low levels in naïve and Hp infected animals at both day 5 and 10 post-infection (Fig. 3). In the serum, proteins levels were similar at both d5 and d10 post-infection at around 2000pg/ml for both Tg and HpTg groups (Fig. 3F). In the SI, IFNγ gene expression increased with infection similarly in Tg and HpTg infected animals, in all regions. The fold increase was below 20-fold at d5, but increased to up to 100-fold by d10 post-infection (Fig. 3A). IFNγ expression levels also increased equally in Tg and HpTg groups in the PP, SPL and LIV (Fig. 3B, D & E). Levels increased by approximately 20 and 50-fold in the SPL and LIV respectively (Fig. 3E & F), while in the PP, the fold increase ranged from approximately 50 to 200 (Fig. 3B). The MLN were the organ with the highest fold increase (approximately 700 at d5 post-infection, Fig. 3C) and the only site with a significant decrease in levels observed at d10 post-infection (down to approximate 150-200 fold, Fig. 3C). Importantly, the only difference observed between Tg and HpTg infected animals was found at d5 post-infection in the MLN (Fig. 3C), where the fold increase in IFNγ in HpTg animals was only a approximately a third of that measured in the Tg-infected group.

The expression of IL-4 and IL-13 in HpTg mice is associated with the Hp profile at day 5 and the Tg profile at d10 in all organs studied except for the MLN, while IL-10 expression in HpTg mice is associated with the Tg profile only

It is known that production of Th2 cytokines can lead to reduced inflammatory responses [45],[46], with IL-4 production directly inhibiting IFNγ production [47]. The Th2 cytokines IL-4, IL-13 and IL-10 are involved in worm expulsion [12],[48]–[50]. In the absence of IL-4 and IL-13, worm expulsion is compromised [50] and high levels of IL-10 have been associated with resistant phenotypes [12]. Interestingly, as well as playing a role during worm infections, IL-10 expression in the SI is required to prevent necrosis and mortality of Tg infected animals [35]. Therefore, we next measured the gene expression of IL-4, IL-13 and IL-10 (Fig. 4 & 5).

Hp adult worms are mostly found in the proximal part of the SI, in close proximity to the stomach [51]. Tg is mostly associated with pathology in the ileum [52],[53], but has been found to replicate all along the SI, both proximal and distal [13]. We analysed IL-4 and IL-13 gene expression in the SI, divided into four equal parts (I1-4, from proximal to distal). At d5 post-infection, IL-4 and IL-13 production was increased in Hp infected animals in all sections (apart from in I4 for IL-13), as expected (Fig 4A). By day 10, levels had significantly increased in all sections; this was most apparent in the proximal sections (I1 & I2, Fig 4A). In Tg infected animals, IL-4 and IL-13 expression was similar to naïve mice in all sections and time points tested (Fig 4A). At day 5, HpTg animals had profiles that resembled Hp animals while at d10, they switched over to the profile observed

in Tg animals. At day 5, IL-4 expression significantly differed between Tg and HpTg mice along most of the small intestine (sections I1, I3 and I4); this was also observed for IL-13 (sections I1, I2 and I3). In section I3, IL-4 expression was highest in HpTg animals. At d10, the Tg and HpTg group cytokine levels remained low and did not differ between any section or time point tested (Fig 4A).

Surprisingly, IL-10 levels were only increased in Tg and HpTg, and not Hp infected groups at both time points in most of the small intestine (sections I1, I2 and I3 (Fig 5A)). Levels at d10 post Tg-infection were greater than at d5 in all sections, and only in I2 at d5 post Tg infection did levels between Tg and HpTg groups differ (levels were extremely low with a mean fold increase of 4.9 +/- 2.4 for the Tg group and 3.5 +/- 1.4 for the HpTg mice). IL-10 levels were not elevated in Hp infected animals at any time point, nor were they in any experimental group in I4.

To analyse whether the IL-4, IL-13 and IL-10 cytokine profiles could be observed outside the SI, we measured IL-4, IL-13 and IL-10 cytokine expression in the PP, MLN, SPL, and LIV (Fig. 4B-E & 5B-E). Like in the SI, levels of IL-4 and IL-13 were increased in all organs (except for IL-13 in the LIV) in Hp infected animals while they remained at naïve levels in Tg infected animals (Fig. 4B-E). HpTg animals had profiles that resembled Hp animals at day 5 but Tg animals at d10. The exceptions were the low levels of IL-13 in the SPL of HpTg mice at d5 and the elevated levels of IL-13 in HpTg mice in the MLN at d10.

For IL-10, levels were increased in all organs at both time points in Tg/HpTg infected animals like in the SI, while they remained at naïve levels in Hp infected animals (Fig. 5B-E). HpTg animals had profiles that resembled Tg animals at both time points. The highest levels were recorded in the PP and SPL at d10 post-infection.

Decreased IFNγ production in the MLN of d5 infected HpTg mice is not specific to a particular cell type and is associated with an increase in GrzmB producing cells.

The MLN are the draining lymph nodes to the SI. Different lymphocytes produce IFNγ within this immune organ, including NK and $CD8^+$ T cells, traditionally associated with IFNγ production during Tg infection [15],[16],[54],[55], as well as NKT, γδ and $CD4^+$ T cell more recently implicated in the inflammatory response to Tg infection [21],[56],[57]. To determine whether a particular cell type was associated with the decrease in IFNγ production observed in HpTg in the MLN at d5 post-Tg infection, we studied cell kinetics and IFNγ production in these five cell types. Compared to the naïve group, MLN cell numbers were increased approximately 4-5 times in all infected groups (Fig. 6A). As expected, percentages of NK, NKT and γδ T cells were low (under 3% approximately), while percentages of $CD4^+$ and $CD8^+$ T cells were much higher (means ranging from 13 to 34%) (Fig. 6B). For all cell types, apart from NK cells, cell percentages and numbers were similar between HpTg and Hp infected animals and different between HpTg and Tg infected animals (Fig. 6B). The percentage and number of NK cells in HpTg infected animals was different to both Hp and Tg groups (Fig. 6B). IFNγ-producing cells are mainly observed in the Tg-infected group. γδ T and NK cells have the highest proportion of IFNγ producers at 12% each (+/- 6.2 and 11

respectively), while the highest number of IFNγ-producing cells are within the $CD8^+$ T cell subset (mean of $5.8x10^5$ cells, +/- $5.7x10^5$). Across all cell types, the percentage and number of IFNγ-producing cells is similar between HpTg and Hp-infected animals, and decreased compared to Tg-infected animals (Fig. 6C). By d10 post-Tg infection, the proportion and number of all IFNγ producing lymphocytes studied in the MLN of HpTg infected are no longer decreased compared to those in Tg-infected mice (data not shown).

Interestingly, the same pattern was not observed for Granzyme B (GrzmB, Fig. 6D). GrzmB, a serine protease that activates apoptosis, has traditionally been associated with NK and $CD8^+$ T cell killing mechanisms, explaining its increase during Tg infection [58]. However, the extent of its role during Tg infection remains controversial. Some studies have shown that Tg can actively inhibit GrzmB in infected cells [59] implying that GrzmB production negatively impacts Tg infection. Others have found GrzmB to have a limited role in host protection [60]. Interestingly, GrzmB is also upregulated during nematode infections, although its precise role (harmful/beneficial to the host) also remains controversial [61]. We observe no increase in the proportion of GrzmB-producing lymphocytes between the HpTg and Tg infected groups in any of the cell types, with NK cells having the largest proportion of GrzmB producers (Fig. 6D). However, the numbers of NK, NKT and $CD4^+$ T cell GrzmB producers were significantly increased in HpTg compared to Tg infected animals (Fig. 6D). By d10 post-Tg infection, the proportion and number of all GrzmB producing lymphocytes studied remain similar between Tg and HpTg mice (data not shown).

In the PP, IFNγ production is only decreased within the CD8$^+$ T cell compartment while GrzmB production is increased in both CD4$^+$ and CD8$^+$ T cells.

The PP are loosely organised lymphoid follicles found along the SI that exhibit differential responses after Hp infection [62]. Tg is also known to infect and replicate within them [63]. Unlike in the MLN, we found no difference between the levels of IFNγ transcripts in the Tg and HpTg groups (Fig 3). However, differential effects on the different IFNγ producing cells could account for this. We therefore studied the percentage of IFNγ-producing lymphocytes within the PP (NK, CD8$^+$ T, NKT, γδ T and CD4$^+$ T) (Fig. 6). Unlike with the MLN, we did not study the cell numbers as the PP are not a discreet organ and the number of cells varies per experiment.

The percentages of all cell types in the HpTg group were similar to the Hp group (Fig. 7, left), which equates to a decrease in T cells (CD8$^+$ T and CD4$^+$ T) and an increase in the NK and NKT cells compared to Tg infected animals (Fig. 7, left). Only the IFNγ-producing CD8$^+$ T cells were decreased in the HpTg group compared to the Tg group (Fig. 7, middle), while both the GrzmB-producing CD8$^+$ and CD4$^+$ cells increased in the HpTg compared to the Tg infected groups (Fig. 7 right). By d10 post-Tg infection, no differences were observed in the PP between the HpTg and Tg groups in any of the parameters studied (data not shown). Differences between the HpTg and Tg groups were not found in any of the IFNγ-producing or the GrzmB-producing lymphocytes in the spleen and/or liver at either time point (data not shown).

DISCUSSION

Early IFNγ production plays a key role in the host defence against *T. gondii*. However, its production can be limited by the Th2 immune profile generated against *H. polygyrus* during co-infections [64]. We set out to determine whether the IFNγ response was affected equally amongst the different lymphocyte producers (NK, $CD8^+$ T, $CD4^+$ T, NKT and γδ T cells) in different organs (SI, PP, MLN, SPL, and LIV). We also studied the impact of these cytokine changes on organ pathology and animal survival.

The PP and the MLN are the local lymphoid organs most involved in the response to intestinal parasites. In both these lymphoid tissues, as well as in the intestine (SI), we found immunological differences between the Tg and HpTg groups. This was not true in other organs more distant from the initial infection site (SPL and LIV). We found an increase in Th2 cytokine levels, IL-4 and IL-13, in HpTg mice in the SI, PP, MLN, and SPL. The differences observed were short-lived, only present in the early stages of co-infection (d5 post-Tg-infection), with the exception of IL-13, which remained upregulated in the MLN of HpTg mice at d10 post-Tg-infection (Fig 3). It is known that IL-4 inhibits the transcription of IFNγ by effector Th1 cells [47]. This was not observed in the distant organs (SPL and LIV) where Th2 cytokines had little impact on the IFNγ production. Our results contradict previous research showing a decrease in splenic IFNγ producing $CD8^+$ T cells in a model of HpTg coinfection [24]. However, this group used irradiated Tg tachyzoites of the RH strain (most virulent strain) injected intra-peritoneally, and measured IFNγ response 7 days post Tg infection. Rh is known to stimulate much stronger IFNγ responses than the Me49 strain used

here [65], and intraperitoneal injection is more likely to stimulate splenic responses than infection by gavage. In contrast, in the lymphoid organs associated with immune responses in the small intestine, the PP and MLN, the presence of Th2 cytokines was associated with a reduction on the proportion of IFNγ-producing lymphocytes (Fig 4, 6 & 7). In the HpTg animals, the proportion of IFNγ producing $CD8^+$ T cells was reduced in the PP (Fig 7) and all IFNγ producing lymphocytes studied (NK, CD8, γδ T, NKT and CD4) were decreased in the MLN, (Fig 6). Our findings are in accordance with previous research finding reduced IFNγ producing $CD4^+$ and $CD8^+$ T cells in the MLN of HpTg mice [23], although this group observed the decrease was still present in $CD8^+$ T cells at a later time point which we did not. Interestingly, when the infections are reversed, Tg inoculated first followed by Hp, no differences between the frequency of $Tbet^+$ or $IFN\gamma^+$ T cells in TgHp and Tg animals have been found [22]. In our hands, the lack of IFNγ producers at d5 post-Tg-infection in the MLN of HpTg mice was associated with high levels of mortality later in infection. This correlates with findings by Khan *et al.* where the IFNγ producing ability of $CD4^+$ T cells after 30 days was associated with survival past 50 days [23].

Increased levels of IL-4 and IL-10 are responsible for the decrease in $IFNg^+$ $CD8^+$ T cells observed in the spleens of HpTg co-infected mice [24]. In contrast, we found that in the presence of IL-10, IFNγ production by $CD8^+$ T cells is not reduced by the co-infection. At d10 post-Tg-infection, increases in IFNγ are correlated to increases in IL-10 (Fig 3 & 5). This was not unexpected since IL-10 is required to limit excessive immunopathology during Tg infection [66]. We were surprised not to see higher levels of IL-10 transcription in Hp infected mice since *in vitro* Ag stimulated lamina propria cells [67] and MLN [11] cells from C57BL/6 Hp infected animals produce IL-10.

However, studies measuring IL-10 transcript levels in the spleen of C57BL/6 mice co-infected with Hp and *Plasmodium chabaudi* found that IL-10 only increased by 2-fold after 7 days of Hp infection which is in line with our findings (Fig 5D). The highest level of Th2 cytokines observed in the gut were in the proximal regions, which coincide with Hp's preferred niche. Despite Hp being entirely enteric, IL-4 (but not IL-13) was detected in sites distal to infection, such as the liver, at both time points. This extends previous findings whereby IL-4 and IL-13 were both previously detected at earlier time points in the liver of infected mice (4 and 7 days post-infection) [68].

Interestingly, studies have also reported that IL-4 production results in increased cytotoxicity in splenic NK cells in the context of Nb infection [69]. Others have found that IL-4 suppresses NK cell cytotoxicity *in vitro* [70]–[72]. We found that GrzmB-producing cells were increased Hp and HpTg groups in the PP and MLN, but not Tg group (Fig 6 & 7). This was surprising because GrzmB is a molecule involved in $CD8^+$ T cell and NK cell cytotoxicity [18],[73]. Despite the increase in cells capable of neutralising Tg-infected cells, the HpTg had worse survival and higher Tg loads than the Tg animals. However, Tg can inhibit GrzmB mediated apoptosis of infected cells [59],[74], which may explain why increased levels of GrzmB expressing cells are not linked with decreased parasite loads in the HpTg animals (Fig 2, 6 & 7). GrzmB expressing lymphocytes were increased in Hp and HpTg infected animals. However, the role of GrzmB during helminth infection is unclear [61] and requires further investigation.

There are few studies examining the impact of Tg infection on organ pathology. We, like others [75], have shown that Tg induces villous blunting, associated with a decrease in goblet cell

numbers (Fig 1B & 1C). Goblet cells are responsible for the production and release of mucins that protect the intestinal epithelium against pathogens. These cells are regulated by IL-4 and IL-13 [76]. During helminth infections, the increase in mucin secretion as a result of goblet cell hyperplasia, helps expel intestinal worms [22],[77]–[83]. While we observed a decrease in goblet cell numbers in Tg infected mice in the proximal small intestine, both HpTg and Hp infected animals had goblet cell hyperplasia (Fig 1B) as well as elevated IL-4 and IL-13 (Fig 2B) in the proximal SI. The regulation of IL-4 and IL-13, and therefore goblet cell hyperplasia has been attributed to T cells, but recent studies demonstrate that NK cell-derived IL-13 has an important role in the induction of goblet cell hyperplasia early in the infection [84]. It is still unclear whether these cell types are responsible for increased Th2 cytokine production during co-infection, as the assessment of $NK1.1^{+}$ derived IL-4 and IL-13 in the SI of Tg and HpTg animals are technically challenging in Hp infected animals. However, further investigation is needed.

Differences in goblet cell numbers therefore do not account for the observed difference in Hp load between Tg and HpTg infected mice (Fig 2A). However, in the HpTg animals, despite elevated IL-4, IL-13 and goblet cell numbers, the increased IL-10/IFNγ levels likely interfered with a more effective anti-worm response (Fig 2A). IFNγ can reduce Th2 cytokine (including IL-4 and IL-13) expression in $CD8^{+}$ T cells *in vivo*, as well as reduce the responsiveness of these cells to IL-4 stimulation [85].

Splenomegaly has recently been observed in mice infected with Me49 at 30 days post-infection, with splenic tissue showing a pro-oxidative and pro-inflammatory profile [86]. Similarly, we

measured increased spleen weights in HpTg compared to Tg infected mice, although the spleen pathology was similar between the two groups (Fig. 1C). Increased splenic levels of IL-10 (Fig. 5D) and IFNγ (Fig. 3D) were associated with splenomegaly as early as d5 post Tg infection, with a high Tg burden (Fig. 2E) and severe pathology by d10 (Fig. 1C). The IL-10 was likely produced by both NK and $CD4^+$ T cells [25], while the IFNγ was mainly produced by $CD4^+$ T cells (data not shown). We did not find any differences between the Tg and HpTg groups in the liver. There was no difference in the liver weights (data not shown) or liver pathology. IL-10 (Fig. 5E) and IFNγ (Fig. 3E) were increased in both groups, while IL-4/IL-13 remained low (Fig 4E). We also found that the number of T cells ($CD8^+$, $CD4^+$, γδ and NKT) were increased at d10 post-infection in the liver (data not shown). Our results agree with previous studies showing increases in T cells in the liver d10 post-Tg infection [87], as well as a general increase in liver pathology, infiltrates and inflammation [88].

The impact of HpTg co-infection on survival remains controversial in the context of helminths and Tg. Some [23] have found that found HpTg co-infection results in improved survival of co-infected mice, while others, like ourselves, report increased mortality in the coinfected group using either Hp (Fig 1A), *N. brasiliensis* [26] or *Schistosoma mansoni* [89]. We found that HpTg animals had increased mortality as well as intestinal pathology compared to Tg infected mice (Fig 1, Sup Table 1) despite elevated IL-10 (Fig 4). From day 7, when mice were infected with Tg, Hp was transitioning from a tissue dwelling to a lumen dwelling phase, resulting in pathology in the proximal small intestine as the worms exit the tissue. This, in association with the necrosis and inflammatory infiltrates caused by Tg likely contributed to the accelerated death of the animals.

The effect of helminth infection on microparasite density varies depending on the species pairs involved. A meta-analysis of several co-infection experiments in laboratory mice reveals that the outcome of co-infections by a helminth parasite and a microparasite, is governed by basic ecological rules [90]. Surprisingly, host genotype, sex, parasite taxa, dose, and infection intervals didn't influence microparasite control during co-infection in this analysis [90], although this has been challenged by other studies (dose: [91], sex: [46],[92],[93]. The main finding suggests that the greater the helminth-induced reduction in microparasite-specific IFNγ, the greater the increase in microparasite density [90]. Our findings are in agreement with this model. The reduced IFNγ production in the MLN of HpTg animals (Fig 3C) is associated with increased Tg parasite density in the MLN (Fig 2D), which in turn correlates with higher mortality. Interestingly, this association between IFNγ and parasite load was only observed in the MLN, which is the main site of the Hp Th2 response. We also found that Hp burden was increased in HpTg animals. While others have not seen this, they have observed increased fecundity in the worms of the HpTg group [22],[94].

Unlike our findings, the data in [23]Khan *et al*., 2008 do not fit the prediction made by the Graham meta-analysis [90]. HpTg infected animals showed improved survival, with lower serum IFNγ levels and Tg burden compared to Tg infected animals. The contradictory results may be explained by a difference in dose. Their main findings were obtained from animals infected with 10 cysts. However, they also performed experiments using 35 Tg cysts and showed that animals receiving a cell transfer of $CD8^+$ T cells obtained from HpTg mice followed by a 35 Tg cyst infection

had worse survival than animals with a cell transfer from naïve animals (0 vs. 30% survival at d16 post infection). These results align with our findings where we used 20 cysts. Similarly, it has been shown that co-infection with 100 cysts of Me49 Tg did not improve the survival of NbTg infected animals compared to Tg infection alone, and did not lead to a change in IFNγ protein levels in restimulated MLN or SPL cells [26].

Another explanation for the differences observed in co-infection outcomes between the different groups is the microbiota of laboratory mice. Evidently, differences in the microbiota of laboratory mice exists between institutes [95],[96]. It is also known that both Hp and Tg alter the host microbiota [97]–[99], and in turn, these changes in the microbiota impact immune responses, such as limiting Th2 immunity to Hp [100]. Therefore, we cannot rule out a key role by the microbiota in these different studies.

Overall, we found a decrease in all IFNγ-producing lymphocytes early post-Tg-infection in HpTg animals, highlighting that both innate and adaptive IFNγ producers were affected by the co-infection. The decrease was associated with increased Th2 cytokines, and increased GrzmB expression. These changes were observed only at sites local to Hp infection, in the SI, PP and MLN. The differences in immune responses in the HpTg compared to the Tg infected, as well as their increased intestinal pathology affected their survival. In early infection, HpTg mice had a similar immune phenotype to the Hp animals. This was reversed by day 10, when HpTg mice exhibited a Tg phenotype. Preliminary results from our lab suggest that that the order of infection may be less important than the spacing between the infections. Animals infected with Tg first,

and Hp second (at day 0, 3 or 5 day post-Hp infection) also showed increased mortality compared to Tg infection alone. This is not true for animals infected with Tg 14 days post Hp infection.

Our results indicate that co-infection with parasites stimulating different arms of the immune system can lead to drastic changes in infection dynamics. Understanding the intricacies of immune responses during co-infections is key to developing models that will provide better translatability to real world situations, where invariably humans, livestock, companion animals and wildlife will be harbouring more than one type of infection.

REFERENCES

1. **Hoarau AOG**, **Mavingui P**, **Lebarbenchon C**. Coinfections in wildlife: Focus on a neglected aspect of infectious disease epidemiology. *PLOS Pathog.* 2020; **16**:e1008790-. Available at: https://doi.org/10.1371/journal.ppat.1008790.

2. **Shen S-S**, **Qu X-Y**, **Zhang W-Z**, **Li J**, **Lv Z-Y**. Infection against infection: parasite antagonism against parasites, viruses and bacteria. *Infect. Dis. Poverty*. 2019; **8**:49. Available at: https://doi.org/10.1186/s40249-019-0560-6.DOI: 10.1186/s40249-019-0560-6.

3. **Graham AL**, **Cattadori IM**, **Lloyd-Smith JO**, **Ferrari MJ**, **Bjørnstad ON**. Transmission consequences of coinfection: cytokines writ large? *Trends Parasitol.* 2007; **23**:284–291.DOI: 10.1016/j.pt.2007.04.005.

4. **Brunton L**, **Hilal-Dandan R**, **Knollmann B**. Goodman and Gilman's The Pharmacological Basis of Therapeutics*, 13th Edition*. 13th ed. USA: McGraw-Hill Education; 2018.

5. **Avramenko RW, Bras A, Redman EM, Woodbury MR, Wagner B, Shury T, Liccioli S, *et al.*** High species diversity of trichostrongyle parasite communities within and between Western Canadian commercial and conservation bison herds revealed by nemabiome metabarcoding. *Parasit. Vectors*. 2018; **11**:299. Available at: https://doi.org/10.1186/s13071-018-2880-y.DOI: 10.1186/s13071-018-2880-y.

6. **Clerc M**, **Devevey G**, **Fenton A**, **Pedersen AB**. Antibodies and coinfection drive variation in nematode burdens in wild mice. *Int. J. Parasitol.* 2018; **48**:785–792.DOI: 10.1016/j.ijpara.2018.04.003.

7. **Cooper PJ, Chico M, Sandoval C, Espinel I, Guevara A, Levine MM, Griffin GE, *et al.*** Human infection with *Ascaris lumbricoides* is associated with suppression of the interleukin-2 response

to recombinant cholera toxin B subunit following vaccination with the live oral cholera vaccine CVD 103-HgR. *Infect. Immun.* 2001; **69**:1574–1580.DOI: 10.1128/IAI.69.3.1574-1580.2001.

8. **Su Z**, **Segura M**, **Stevenson MM**. Reduced protective efficacy of a blood-stage malaria vaccine by concurrent nematode infection. *Infect. Immun.* 2006; **74**:2138–2144.DOI: 10.1128/IAI.74.4.2138-2144.2006.

9. **Koboziev I**, **Karlsson F**, **Grisham MB**. Gut-associated lymphoid tissue, T cell trafficking, and chronic intestinal inflammation. *Ann. N. Y. Acad. Sci.* 2010; **1207**.DOI: 10.1111/j.1749-6632.2010.05711.x.

10. **Reynolds LA**, **Filbey KJ**, **Maizels RM**. Immunity to the model intestinal helminth parasite *Heligmosomoides polygyrus*. *Semin. Immunopathol.* 2012; **34**:829–846.DOI: 10.1007/s00281-012-0347-3.

11. **Smith KA, Filbey KJ, Reynolds LA, Hewitson JP, Harcus Y, Boon L, Sparwasser T, *et al.*** Low-level regulatory T-cell activity is essential for functional type-2 effector immunity to expel gastrointestinal helminths. *Mucosal Immunol.* 2016; **9**:428–443.DOI: 10.1038/mi.2015.73.

12. **Filbey KJ, Grainger JR, Smith KA, Boon L, Van Rooijen N, Harcus Y, Jenkins S, *et al.*** Innate and adaptive type 2 immune cell responses in genetically controlled resistance to intestinal helminth infection. *Immunol. Cell Biol.* 2014; **92**:436–448.DOI: 10.1038/icb.2013.109.

13. **Gregg B, Taylor BC, John B, Tait-Wojno ED, Girgis NM, Miller N, Wagage S, *et al.*** Replication and distribution of *Toxoplasma gondii* in the small intestine after oral infection with tissue cysts. *Infect. Immun.* 2013; **81**:1635–1643.DOI: 10.1128/IAI.01126-12.

14. **Denkers EY**, **Icardo R**, **Gazzinelli T**, **Martin D**, **Sher A**. Emergence of NKI.1 + Cells as Effectors of IFN-3' Dependent Immunity to *Toxoplasma gondii* in MHC Class I-deficient Mice. *J. Exp. Med.*

1993; **178**:1465–1472.DOI: DOI: 10.1084/jem.178.5.1465.

15. **Sher A**, **Oswald IP**, **Hieny S**, **Gazzinelli RT**. *Toxoplasma gondii* Induces a T-Independent IFN-)/ Response in Natural Killer Cells That Requires Both Adherent Accessory Cells and Tumor Necrosis Factor-a. *J. Immunol.* 1993; **150**:3982–3989.

16. **Goldszmid RS, Caspar P, Rivollier A, White S, Dzutsev A, Hieny S, Kelsall B, *et al.*** NK Cell-Derived Interferon-γ Orchestrates Cellular Dynamics and the Differentiation of Monocytes into Dendritic Cells at the Site of Infection. *Immunity*. 2012; **36**:1047–1059.DOI: 10.1016/j.immuni.2012.03.026.

17. **Combe CL**, **Curiel TJ**, **Moretto MM**, **Khan I a**. NK Cells Help To Induce CD8 ƨ -T-Cell Immunity against *Toxoplasma gondii* in the Absence of CD4 ƨ T Cells. *Society*. 2005; **73**:4913–4921.DOI: 10.1128/IAI.73.8.4913.

18. **Nakano Y, Hisaeda H, Sakai T, Zhang M, Maekawa Y, Zhang T, Nishitani M, *et al.*** Granule-dependent killing of *Toxoplasma gondii* by CD8 + T cells. *Immunology*. 2001; **104**:289–298.DOI: 10.1046/j.1365-2567.2001.01319.x.

19. **Kasper LH**, **Matsuura T**, **Fonseka S**, **Arruda J**, **Channon JY**, **Khan IA**. Induction of gammadelta T cells during acute murine infection with *Toxoplasma gondii*. *J. Immunol.* 1996; **157**:5521. Available at: http://www.jimmunol.org/content/157/12/5521.abstract.

20. **Ronet C, Darche S, de Moraes ML, Miyake S, Yamamura T, Louis JA, Kasper LH, *et al.*** NKT Cells Are Critical for the Initiation of an Inflammatory Bowel Response against *Toxoplasma gondii* . *J. Immunol.* 2005; **175**:899–908.DOI: 10.4049/jimmunol.175.2.899.

21. **Nakano Y, Hisaeda H, Sakai T, Ishikawa H, Zhang M, Maekawa Y, Zhang T, *et al.*** Roles of NKT cells in resistance against infection with *Toxoplasma gondii* and in expression of heat shock

protein 65 in the host macrophages. *Microbes Infect.* 2002; **4**:1–11. Available at: https://www.sciencedirect.com/science/article/pii/S1286457901015039.DOI: https://doi.org/10.1016/S1286-4579(01)01503-9.

22. **Ahmed N, French T, Rausch S, Kühl A, Hemminger K, Dunay IR, Steinfelder S, *et al.*** *Toxoplasma* Co-infection Prevents Th2 Differentiation and Leads to a Helminth-Specific Th1 Response. *Front. Cell. Infect. Microbiol.* 2017; **7**.DOI: 10.3389/fcimb.2017.00341.

23. **Khan IA**, **Hakak R**, **Eberle K**, **Sayles P**, **Weiss LM**, **Urban JF**. Coinfection with Heligmosomoides polygyrus fails to establish CD8 + T-cell immunity against *Toxoplasma gondii.* *Infect. Immun.* 2008; **76**:1305–1313.DOI: 10.1128/IAI.01236-07.

24. **Marple A**, **Wu W**, **Shah S**, **Zhao Y**, **Du P**, **Gause WC**, **Yap GS**. Cutting Edge: Helminth Coinfection Blocks Effector Differentiation of CD8 T Cells through Alternate Host Th2- and IL-10–Mediated Responses. *J. Immunol.* 2017; **198**:634–639.DOI: 10.4049/jimmunol.1601741.

25. **Perona-Wright G, Mohrs K, Szaba FM, Kummer LW, Madan R, Karp CL, Johnson LL, *et al.*** Systemic but Not Local Infections Elicit Immunosuppressive IL-10 Production by Natural Killer Cells. *Cell Host Microbe*. 2009; **6**:503–512.DOI: 10.1016/j.chom.2009.11.003.

26. **Liesenfeld O**, **Dunay IR**, **Erb KJ**. Infection with *Toxoplasma gondii* reduces established and developing Th2 responses induced by Nippostrongylus brasiliensis infection. *Infect. Immun.* 2004; **72**:3812–3822.DOI: 10.1128/IAI.72.7.3812-3822.2004.

27. **Coomes SM, Pelly VS, Kannan Y, Okoye IS, Czieso S, Entwistle LJ, Perez-Lloret J, *et al.*** IFNγ and IL-12 Restrict Th2 Responses during Helminth/*Plasmodium* Co-Infection and Promote IFNγ from Th2 Cells. *PLoS Pathog.* 2015; **11**.DOI: 10.1371/journal.ppat.1004994.

28. **Shi Y, Zhang P, Wang G, Liu X, Sun X, Zhang X, Li H, *et al.*** Description of organ-specific

phenotype, and functional characteristics of tissue resident lymphocytes from liver transplantation donor and research on immune tolerance mechanism of liver. *Oncotarget*. 2018; **9**:15552–15565. Available at: www.oncotarget.comwww.oncotarget.com.

29. **Pfaffl MW**. Relative quantification. In: *Relative quantification*. CRC Press; 2007:63–82.

30. **Costa JM**, **Bretagne S**. Variation of B1 gene and AF146527 repeat element copy numbers according to *Toxoplasma gondii* strains assessed using real-time quantitative PCR. *J. Clin. Microbiol.* 2012; **50**:1452–1454.DOI: 10.1128/JCM.06514-11.

31. **Cossarizza A, Chang HD, Radbruch A, Acs A, Adam D, Adam-Klages S, Agace WW, *et al.*** Guidelines for the use of flow cytometry and cell sorting in immunological studies (second edition). *Eur. J. Immunol.* 2019; **49**:1457–1973.

32. **Bryant V**. The Life Cycle of *Nematospiroides dubius* , Baylis, 1926 (Nematoda: Heligmosomidae). *J. Helminthol.* 1973; **47**.DOI: 10.1017/S0022149X00026535.

33. **Dubey JP**. Bradyzoite-induced murine toxoplasmosis: stage conversion, pathogenesis, and tissue cyst formation in mice fed bradyzoites of different strains of *Toxoplasma gondii*. *J. Eukaryot. Microbiol.* 1997; **44**:592–602. Available at: http://www.ncbi.nlm.nih.gov/pubmed/9435131 [Accessed June 25, 2015].

34. **Zenner L**, **Darcy F**, **Capron A**, **Cesbron-Delauw M-F**. Toxoplasma gondii: Kinetics of the Dissemination in the Host Tissues during the Acute Phase of Infection of Mice and Rats. *Exp. Parasitol.* 1998; **90**:86–94.

35. **Suzuki Y, Sher A, Yap G, Park D, Neyer LE, Liesenfeld O, Fort M, *et al.*** IL-10 Is Required for Prevention of Necrosis in the Small Intestine and Mortality in Both Genetically Resistant BALB/c and Susceptible C57BL/6 Mice Following Peroral Infection with *Toxoplasma gondii* . *J. Immunol.*

2000; **164**:5375–5382.DOI: 10.4049/jimmunol.164.10.5375.

36. **Specian RD**, **Oliver MG**. Functional biology of intestinal goblet cells. *Am. J. Physiol. Physiol.* 1991; **260**:C183–C193. Available at: https://doi.org/10.1152/ajpcell.1991.260.2.C183.DOI: 10.1152/ajpcell.1991.260.2.C183.

37. **Hunter CA**, **Subauste CS**, **Van Cleave VH**, **Remington JS**. Production of gamma interferon by natural killer cells from *Toxoplasma gondii*-infected SCID mice: regulation by interleukin-10, interleukin-12, and tumor necrosis factor alpha. *Infect. Immun.* 1994; **62**:2818–24. Available at: http://www.pubmedcentral.nih.gov/articlerender.fcgi?artid=302887&tool=pmcentrez&rendertype=abstract [Accessed September 10, 2015].

38. **Khan IA, Thomas SY, Moretto MM, Lee FS, Islam SA, Combe C, Schwartzman JD, *et al.*** CCR5 is essential for NK cell trafficking and host survival following *Toxoplasma gondii* infection. *PLoS Pathog.* 2006; **2**:0484–0500.DOI: 10.1371/journal.ppat.0020049.

39. **Suzuki Y**, **Orellana M**, **Schreiber R**, **Remington J**. Interferon-gamma: the major mediator of resistance against *Toxoplasma gondii. Science (80-.).* 1988; **240**:516–518.DOI: 10.1126/science.3128869.

40. **Suzuki Y**, **Sa Q**, **Gehman M**, **Ochiai E**. Interferon-gamma- and perforin-mediated immune responses for resistance against *Toxoplasma gondii* in the brain. *Expert Rev. Mol. Med.* 2011; **13**.DOI: 10.1017/s1462399411002018.

41. **Scharton-Kersten TM, Wynn TA, Denkers EY, Bala S, Grunvald E, Hieny S, Gazzinelli RT, *et al.*** In the absence of endogenous IFN-gamma, mice develop unimpaired IL-12 responses to *Toxoplasma gondii* while failing to control acute infection. *J. Immunol.* 1996; **157**:4045. Available at: http://www.jimmunol.org/content/157/9/4045.abstract.

42. **Suzuki Y**, **Remington JS**. against toxoplasmosis in mice. protective effect of Lyt-2+ immune T cells The effect of anti-IFN-gamma antibody on the. *J. Immunol.* 1990; **144**:1954–1956. Available at: http://www.jimmunol.org/content/144/5/1954.

43. **Norose K, Mun HS, Aosai F, Chen M, Piao LX, Kobayashi M, Iwakura Y, *et al.*** IFN-γ-regulated *Toxoplasma gondii* distribution and load in the murine eye. *Investig. Ophthalmol. Vis. Sci.* 2003; **44**:4375–4381.DOI: 10.1167/iovs.03-0156.

44. **Dimier IH**. Interferon-γ-activated primary enterocytes inhibit *Toxoplasma gondii* replication: a role for intracellular iron. *Immunology*. 1998; **94**:488–495.

45. **Paludan SR**, **Lovmand J**, **Ellermann-Eriksen S**, **Mogensen SC**. Effect of IL-4 and IL-13 on IFN-*γ* -induced production of nitric oxide in mouse macrophages infected with herpes simplex virus type 2. *FEBS Lett.* 1997; **414**.DOI: 10.1016/S0014-5793(97)00987-3.

46. **Klein SA, Dobmeyer JM, Dobmeyer TS, Pape M, Ottmann OG, Helm EB, Hoelzer D, *et al.*** Demonstration of the Th1 to Th2 cytokine shift during the course of HIV-1 infection using cytoplasmic cytokine detection on single cell level by flow cytometry. *AIDS*. 1997; **11**. Available at: https://journals.lww.com/aidsonline/Fulltext/1997/09000/Demonstration_of_the_Th1_to_Th2_cytokine_shift.5.aspx.

47. **Wurtz O**, **Bajénoff M**, **Guerder S**. IL-4-mediated inhibition of IFN-γ production by CD4+ T cells proceeds by several developmentally regulated mechanisms. *Int. Immunol.* 2004; **16**:501–508. Available at: https://doi.org/10.1093/intimm/dxh050.DOI: 10.1093/intimm/dxh050.

48. **Mckenzie GJ**, **Fallon PG**, **Emson CL**, **Grencis RK**, **Mckenzie ANJ**. Simultaneous Disruption of Interleukin (IL)-4 and IL-13 Defines Individual Roles in T Helper Cell Type 2-mediated Responses.

J. Exp. Med. 1999; **189**:1565–1572. Available at: http://www.jem.org.

49. **Urban JF**, **Noben-Trauth N**, **Donaldson DD**, **Madden KB**, **Morris SC**, **Collins M**, **Finkelman FD**. IL-13, IL-4R, and Stat6 Are Required for the Expulsion of the Gastrointestinal Nematode Parasite *Nippostrongylus brasiliensis* either parasite, disruption of the IL-4 gene or inhibition of IL-4 with an antibody that blocks IL-4 receptor chain (IL-4R) funct. *Immunity*. 1998; **8**:255–264.

50. **Oeser K**, **Schwartz C**, **Voehringer D**. Conditional IL-4/IL-13-deficient mice reveal a critical role of innate immune cells for protective immunity against gastrointestinal helminths. *Mucosal Immunol.* 2015; **8**:672–682.DOI: 10.1038/mi.2014.101.

51. **Lewis JW**, **Bryant V**. The distribution of nematospiroides dubiiis within the small intestine of laboratory mice. *J. Helminthol.* 1976; **50**:163–171.DOI: 10.1017/S0022149X00027693.

52. **SPEER CA**, **DUBEY JP**. Ultrastructure of early stages of infections in mice fed *Toxoplasma gondii* oocysts. *Parasitology*. 1998; **116**:35–42. Available at: https://www.cambridge.org/core/article/ultrastructure-of-early-stages-of-infections-in-mice-fed-toxoplasma-gondii-oocysts/0C77033B895AF448523CE81B742E9CA5.DOI: DOI: 10.1017/S0031182097001959.

53. **Dubey JP**, **Ferreira LR**, **Martins J**, **Mcleod R**. Oral oocyst-induced mouse model of toxoplasmosis: Effect of infection with *Toxoplasma gondii* strains of different genotypes, dose, and mouse strains (transgenic, out-bred, in-bred) on pathogenesis and mortality. *Parasitology*. 2012; **139**:1–13.DOI: 10.1017/S0031182011001673.

54. **Denkers EY**, **Sher A**, **Gazzinelli RT**. CD8+ T-cell interactions with *Toxoplasma gondii*: implications for processing of antigen for class-I-restricted recognition. *Res. Immunol.* 1993; **144**:51–57. Available at:

https://www.sciencedirect.com/science/article/pii/S0923249405800999.DOI: https://doi.org/10.1016/S0923-2494(05)80099-9.

55. **Khan IA**, **Green WR**, **Kasper LH**, **Green KA**, **Schwartzman JD**. Immune CD8+ T Cells Prevent Reactivation of *Toxoplasma gondii* Infection in the Immunocompromised Host. *Infect. Immun.* 1999; **67**.DOI: 10.1128/IAI.67.11.5869-5876.1999.

56. **Edelblum KL, Singh G, Odenwald MA, Lingaraju A, El Bissati K, McLeod R, Sperling AI, *et al.*** γδ intraepithelial lymphocyte migration limits transepithelial pathogen invasion and systemic disease in mice. *Gastroenterology*. 2015; **148**:1417–1426.DOI: 10.1053/j.gastro.2015.02.053.

57. **Khan IA**, **Hwang S**, **Moretto M**. *Toxoplasma gondii*: CD8 T cells cry for CD4 help. *Front. Cell. Infect. Microbiol.* 2019; **9**.DOI: 10.3389/fcimb.2019.00136.

58. **Bhadra R**, **Gigley JP**, **Khan IA**. The CD8 T-cell road to immunotherapy of toxoplasmosis. *Immunotherapy*. 2011; **3**:789–801.DOI: 10.2217/imt.11.68.

59. **Yamada T**, **Tomita T**, **Weiss LM**, **Orlofsky A**. *Toxoplasma gondii* inhibits granzyme B-mediated apoptosis by the inhibition of granzyme B function in host cells. *Int. J. Parasitol.* 2011; **41**:595–607.DOI: 10.1016/j.ijpara.2010.11.012.

60. **Denkers EY, Yap G, Scharton-Kersten T, Charest H, Butcher BA, Caspar P, Heiny S, *et al.*** Perforin-Mediated Cytolysis Plays a Limited Role in Host Resistance to *Toxoplasma gondii. J. Immunol.* 1997; **159**:1903–1904. Available at: http://www.jimmunol.org/.

61. **Fujiwara A**, **Kawai Y**, **Sekikawa S**, **Horii T**, **Yamada M**, **Mitsufuji S**, **Arizono N**. Villus epithelial injury induced by infection with the nematode *Nippostrongylus brasiliensis* is associated with upregution of Granzyme B V. *J. Parasitol.* 2004; **90**:1019–1026. Available at: https://doi.org/10.1645/GE-265R.DOI: 10.1645/GE-265R.

62. **Mosconi I, Dubey LK, Volpe B, Esser-von Bieren J, Zaiss MM, Lebon L, Massacand JC, *et al.*** Parasite proximity drives the expansion of regulatory T cells in Peyer's patches following intestinal helminth infection. *Infect. Immun.* 2015; **83**:3657–3665.DOI: 10.1128/IAI.00266-15.

63. **Mitsunaga T**, **Norose K**, **Aosai F**, **Horie H**, **Ohnuma N**, **Yano A**. Infection dynamics of *Toxoplasma gondii* in gut-associated tissues after oral infection: The role of Peyer's patches. *Parasitol. Int.* 2019; **68**:40–47. Available at: https://www.sciencedirect.com/science/article/pii/S1383576917304853.DOI: https://doi.org/10.1016/j.parint.2018.08.010.

64. **Olguín JE, Fernández J, Salinas N, Juárez I, Rodriguez-Sosa M, Campuzano J, Castellanos C, *et al.*** Adoptive transfer of CD4+Foxp3+ regulatory T cells to C57BL/6J mice during acute infection with *Toxoplasma gondii* down modulates the exacerbated Th1 immune response. *Microbes Infect.* 2015; **17**:586–595.DOI: 10.1016/j.micinf.2015.04.002.

65. **Gavrilescu LC**, **Denkers EY**. IFN-γ Overproduction and High Level Apoptosis Are Associated with High but Not Low Virulence *Toxoplasma gondii* Infection . *J. Immunol.* 2001; **167**:902–909.DOI: 10.4049/jimmunol.167.2.902.

66. **Gazzinelli RT, Wysocka M, Hieny S, Scharton-Kersten T, Cheever A, Kuhn R, Muller W, *et al.*** In the Absence of Endogenous IL-10, Mice Acutely Infected with *Toxoplasma gondii* Succumb to a Lethal immune Response Dependent on CD4+ T Cells and Accompanied by Overproduction of 11-12, IFN-γ, and TNF-cw. *J. Immunol.* 1996; **157**:798–805.

67. **Setiawan T**, **Metwali A**, **Blum AM**, **Ince MN**, **Urban JF**, **Elliott DE**, **Weinstock J V.** *Heligmosomoides polygyrus* promotes regulatory T-cell cytokine production in the murine normal distal intestine. *Infect. Immun.* 2007; **75**:4655–4663.DOI: 10.1128/IAI.00358-07.

68. **Helmby H**. Gastrointestinal Nematode Infection Exacerbates Malaria-Induced Liver Pathology. *J. Immunol.* 2009; **182**:5663–5671.DOI: 10.4049/jimmunol.0803790.

69. **Kiniwa T**, **Enomoto Y**, **Terazawa N**, **Omi A**, **Miyata N**, **Ishiwata K**, **Miyajima A**. NK cells activated by Interleukin-4 in cooperation with Interleukin-15 exhibit distinctive characteristics. *Proc. Natl. Acad. Sci.* 2016; **113**:10139–10144. Available at: https://www.pnas.org/content/113/36/10139 [Accessed May 22, 2021].DOI: 10.1073/PNAS.1600112113.

70. **Brady J**, **Carotta S**, **Thong RPL**, **Chan CJ**, **Hayakawa Y**, **Smyth MJ**, **Nutt SL**. The Interactions of Multiple Cytokines Control NK Cell Maturation. *J. Immunol.* 2010; **185**:6679–6688.DOI: 10.4049/jimmunol.0903354.

71. **Bratke K**, **Goettsching H**, **Kuepper M**, **Geyer S**, **Luttmann W**, **Virchow JC**. Interleukin-4 suppresses the cytotoxic potential of *in vitro* generated, adaptive regulatory CD4+ T cells by down-regulation of granzyme B. *Immunology*. 2009; **127**:338–344.DOI: 10.1111/j.1365-2567.2008.02993.x.

72. **Ohayon D**, **Krishnamurthy D**, **Brusilovsky M**, **Waggoner S**. IL-4 and IL-13 modulate natural killer cell responses under inflammatory conditions. *J. Immunol.* 2017; **198**:194.

73. **Dotiwala F, Mulik S, Polidoro RB, Ansara JA, Burleigh BA, Walch M, Gazzinelli RT, *et al.*** Killer lymphocytes use granulysin, perforin and granzymes to kill intracellular parasites. *Nat. Med.* 2016; **22**:210–216.DOI: 10.1038/nm.4023.

74. **Nash P**, **Purner M**, **Leon R**, **Clarke P**, **Duke R**, **Curiel T**. *Toxoplasma gondii*-Infected Cells Are Resistant to Multiple Inducers of Apoptosis. *J. Immunol.* 1998; **160**:1824–1830.

75. **Jensen KDC, Wang Y, Wojno EDT, Shastri AJ, Hu K, Cornel L, Boedec E, *et al.*** Toxoplasma

polymorphic effectors determine macrophage polarization and intestinal inflammation. *Cell Host Microbe*. 2011; **9**:472–483. Available at: https://pubmed.ncbi.nlm.nih.gov/21669396.DOI: 10.1016/j.chom.2011.04.015.

76. **Hashimoto K**, **Uchikawa R**, **Tegoshi T**, **Takeda K**, **Yamada M**, **Arizono N**. Depleted intestinal goblet cells and severe pathological changes in SCID mice infected with *Heligmosomoides polygyrus*. *Parasite Immunol.* 2009; **31**:457–465.DOI: 10.1111/j.1365-3024.2009.01123.x.

77. **Bogers**, **Moreels**, **De Man**, **Vrolix**, **Jacobs**, **Pelckmans**, **Van Marck**. *Schistosoma mansoni* infection causing diffuse enteric inflammation and damage of the enteric nervous system in the mouse small intestine. *Neurogastroenterol. Motil.* 2000; **12**.DOI: 10.1046/j.1365-2982.2000.00219.x.

78. **Balemba OB**, **Semuguruka WD**, **Hay-Schmidt A**, **Johansen M V**, **Dantzer V**. Vasoactive intestinal peptide and substance P-like immunoreactivities in the enteric nervous system of the pig correlate with the severity of pathological changes induced by Schistosoma japonicum. *Int. J. Parasitol.* 2001; **31**:1503–1514. Available at: https://www.sciencedirect.com/science/article/pii/S0020751901002739.DOI: https://doi.org/10.1016/S0020-7519(01)00273-9.

79. **Buzoni-Gatel D**, **Werts C**. *Toxoplasma gondii* and subversion of the immune system. *Trends Parasitol.* 2006; **22**:448–452. Available at: https://doi.org/10.1016/j.pt.2006.08.002.DOI: 10.1016/j.pt.2006.08.002.

80. **KNIGHT PA**, **BROWN JK**, **PEMBERTON AD**. Innate immune response mechanisms in the intestinal epithelium: potential roles for mast cells and goblet cells in the expulsion of adult *Trichinella spiralis*. *Parasitology*. 2008; **135**.DOI: 10.1017/S0031182008004319.

81. **Marillier RG, Michels C, Smith EM, Fick LCE, Leeto M, Dewals B, Horsnell WGC, *et al.*** IL-4/IL-13 independent goblet cell hyperplasia in experimental helminth infections. *BMC Immunol.* 2008; **9**:11. Available at: https://pubmed.ncbi.nlm.nih.gov/18373844.DOI: 10.1186/1471-2172-9-11.

82. **Artis D, Wang ML, Keilbaugh SA, He W, Brenes M, Swain GP, Knight PA, *et al.*** RELM /FIZZ2 is a goblet cell-specific immune-effector molecule in the gastrointestinal tract. *Proc. Natl. Acad. Sci.* 2004; **101**.DOI: 10.1073/pnas.0404034101.

83. **Owyang AM, Zaph C, Wilson EH, Guild KJ, McClanahan T, Miller HRP, Cua DJ, *et al.*** Interleukin 25 regulates type 2 cytokine-dependent immunity and limits chronic inflammation in the gastrointestinal tract. *J. Exp. Med.* 2006; **203**.DOI: 10.1084/jem.20051496.

84. **McDermott JR**, **Humphreys NE**, **Forman SP**, **Donaldson DD**, **Grencis RK**. Intraepithelial NK Cell-Derived IL-13 Induces Intestinal Pathology Associated with Nematode Infection. *J. Immunol.* 2005; **175**:3207–3213.DOI: 10.4049/jimmunol.175.5.3207.

85. **Apte SH**, **Groves P**, **Olver S**, **Baz A**, **Doolan DL**, **Kelso A**, **Kienzle N**. IFN-γ Inhibits IL-4–Induced Type 2 Cytokine Expression by CD8 T Cells *In Vivo* and Modulates the Anti-Tumor Response. *J. Immunol.* 2010; **185**:998–1004.DOI: 10.4049/jimmunol.0903372.

86. **Doleski PH, Ten Caten M V, Passos DF, Castilhos LG, Leal DBR, Machado VS, Bottari NB, *et al.*** Toxoplasmosis treatment with diphenyl diselenide in infected mice modulates the activity of purinergic enzymes and reduces inflammation in spleen. *Exp. Parasitol.* 2017; **181**:7–13. Available at: https://www.sciencedirect.com/science/article/pii/S0014489416303940.DOI: https://doi.org/10.1016/j.exppara.2017.07.001.

87. **Heimesaat MM**, **Mrazek K**, **Bereswill S**. Murine fecal microbiota transplantation lowers

gastrointestinal pathogen loads and dampens pro-inflammatory immune responses in *Campylobacter jejuni* infected secondary abiotic mice. *Sci. Rep.* 2019; **9**.DOI: 10.1038/s41598-019-56442-7.

88. **Cavalcanti MG**, **Mesquita JS**, **Madi K**, **Feijó DF**, **Assunção-Miranda I**, **Souza HSP**, **Bozza MT**. MIF Participates in *Toxoplasma gondii*-Induced Pathology Following Oral Infection. *PLoS One*. 2011; **6**.DOI: 10.1371/journal.pone.0025259.

89. **Marshall AJ**, **Brunet LR**, **van Gessel Y**, **Alcaraz A**, **Bliss SK**, **Pearce EJ**, **Denkers EY**. *Toxoplasma gondii* and *Schistosoma mansoni* synergize to promote hepatocyte dysfunction associated with high levels of plasma TNF-alpha and early death in C57BL/6 mice. *J. Immunol.* 1999; **163**:2089–97.

90. **Graham AL**. Ecological rules governing helminth-microparasite coinfection. *Proc. Natl. Acad. Sci. U. S. A.* 2008; **105**:566–570. Available at: www.pnas.org/cgi/content/full/.DOI: 10.1073/pnas.0707221105.

91. **Fellous S**, **Koella JC**. Infectious dose affects the outcome of the within-host competition between parasites. *Am. Nat.* 2009; **173**.DOI: 10.1086/598490.

92. **Thompson O**, **Gipson SAY**, **Hall MD**. The impact of host sex on the outcome of co-infection. *Sci. Rep.* 2017; **7**.DOI: 10.1038/s41598-017-00835-z.

93. **Roberts CW**, **Cruickshank SM**, **Alexander J**. Sex-determined resistance to *Toxoplasma gondii* is associated with temporal differences in cytokine production. *Infect. Immun.* 1995; **63**:2549–2555.

94. **French T, Düsedau HP, Steffen J, Biswas A, Ahmed N, Hartmann S, Schüler T, *et al.*** Neuronal impairment following chronic Toxoplasma gondii infection is aggravated by intestinal

nematode challenge in an IFN-γ-dependent manner. *J. Neuroinflammation*. 2019; **16**.DOI: 10.1186/s12974-019-1539-8.

95. **Hirayama K**, **Endo K**, **Kawamura S**, **Mitsuoka T**. Comparison of the Intestinal Bacteria in Specific Pathogen Free Mice from Different Breeders. *Exp. Anim*. 1990; **39**:263–267.

96. **Alegre ML**. Mouse microbiomes: Overlooked culprits of experimental variability. *Genome Biol.* 2019; **20**.DOI: 10.1186/s13059-019-1723-2.

97. **Walk ST**, **Blum AM**, **Ewing SAS**, **Weinstock J V.**, **Young VB**. Alteration of the murine gut microbiota during infection with the parasitic helminth *Heligmosomoides polygyrus*. *Inflamm. Bowel Dis.* 2010; **16**:1841–1849.DOI: 10.1002/ibd.21299.

98. **Prandovszky E, Li Y, Sabunciyan S, Steinfeldt CB, Avalos LN, Gressitt KL, White JR, *et al.*** *Toxoplasma gondii*-induced long-term changes in the upper intestinal microflora during the chronic stage of infection. *Scientifica (Cairo).* 2018; **2018**.DOI: 10.1155/2018/2308619.

99. **Shao DY, Bai X, Tong MW, Zhang Y yuan, Liu X lei, Zhou Y hua, Li C, *et al.*** Changes to the gut microbiota in mice induced by infection with *Toxoplasma gondii*. *Acta Trop.* 2020; **203**.DOI: 10.1016/j.actatropica.2019.105301.

100. **Russell GA**, **Faubert C**, **Verdu EF**, **King IL**. The gut microbiota limits Th2 immunity to *Heligmosomoides polygyrus bakeri* infection. *bioRxiv*. 2020.DOI: 10.1101/2020.01.30.927111.

FIGURE LEGENDS

Figure 1: ***H. polygyrus co-infection leads to high mortality and pathology in mice co-infected with Toxoplasma gondii.*** 200 Hp larvae were given to mice 7 days prior to infection with 20 Tg tissue cysts. A. Survival was measured for 16 days post Tg infection. N = 4 mice (Tg and HpTg-infected groups) and 2-4 mice (naïve/Hp-infected groups) per experiment, 3 independent experiments. Mantel-Cox test performed for pooled data, *p=0.02 (Tg vs. HpTg). B. Small intestines were harvested from mice 5 and 10 days post Tg infection, and formalin fixed. 6uM slides were cut from the paraffin embedded swiss rolls, and stained with hematoxylin and eosin (top) or Alcian blue (bottom). Representative photographs are from each experimental group and each time point Scale: 1mm top and 50um bottom. Black arrows depict granulomas (Hp pathology) and white arrows depict leukocyte infiltrates (Tg pathology). Top right, average villi perimeter in the proximal small intestine of each experimental group on day 5 post Tg infection. The perimeter of 5 intact continuous villi was measured and averaged. N= 2-4 mice per group per experiment, 2 independent experiments. Anderson-Darling normality test followed by ANOVA were performed for pooled data, n.s. = non significant, * = $p<0.05$. Bottom right, average number of goblet cells in 5 intact and continuous villi within the proximal small intestine of each experimental group on day 5 post Tg infection. N= 2-4 mice per group per experiment, 2 independent experiments. Normality test followed by ANOVA was performed for pooled data, n.s. = non significant, ** = $p<0.01$. Spleens (C) and livers (D) were harvested from mice 5 and 10 days post Tg infection, and formalin fixed. 6uM slides were cut from the paraffin embedded tissue and stained with hematoxylin and eosin. Representative photographs are

from each experimental group and each time point. Scale: 10um. White arrows depict leukocyte infiltrates (Tg pathology). Average spleen (C) and liver (D) pathology score for each mouse, euthanized at day 5 (middle) and 10 (right) post Tg infection. N= 3-7 mice per group per experiment, 2 independent experiments. Anderson-Darling normality test followed by ANOVA were performed for pooled data, n.s. = non significant, ** = $p<0.01$ and *** = $p<0.001$.

Figure 2: ***Parasite burdens differ between HpTg and Tg in the small intestine and the MLN.*** 200 Hp larvae were given to mice 7 days prior to infection with 20 Tg tissue cysts. (A) Adult worms were counted in the small intestine of Hp and HpTg infected mice at 5 (left) and 10 (right) days post Tg infection (12 and 17 days post Hp infection). Data were tested for normality (Anderson-Darling test). Students' T and/or Mann-Whitney tests were performed on parametric/non-parametric pooled data for each time point (D5 and D10), * = $p<0.05$, and ***= $p<0.001$. (B-F) Tg loads were measured by quantitative RT-PCR in the small intestine (B), Peyers patches (C), mesenteric lymph nodes (D), spleen (E) and liver (F) at 5 (left) and 10 (right) days post -infection. N= 2-6 mice per group per experiment, 2 independent experiments. Data was tested for normality (Anderson-Darling test). T-tests/Mann Whitney tests were performed on parametric/non-parametric pooled data on either Hp vs. HpTg or Tg vs. HpTg; n.s. = non significant and ***= $p<0.001$.

Figure 3: ***IFNγ gene expression profile in HpTg infected mice mirrors that of Tg infected mice except in the MLN at d5 post infection.*** 200 Hp larvae were given to mice 7 days prior to infection with 20 Tg tissue cysts. IFNγ gene expression was measured by quantitative RT-PCR in the small intestine (A), the Peyer's Patches (B), the mesenteric lymph nodes (C), the spleen (D) and the liver (E) at 5 (left) and 10 (right) days post -infection. IFNγ protein levels were measured in the serum by ELISA (F). N= 2-4 mice per group per experiment, a minimum of 2 independent experiments. Data was tested for normality (Anderson-Darling test). ANOVA or Kriskal-Wallis tests were performed on parametric/non-parametric pooled data, and when significant, Sidak's/Dunn's Multiple comparisons were performed on Hp vs. HpTg and Tg vs. HpTg; n.s. = non significant, * = $p<0.05$, ** = $p<0.01$, ***= $p<0.001$ and ****= $p<0.0001$.

Figure 4: ***IL-4 and IL-13 gene expression profiles in HpTg infected mice mirror those of Hp infected mice at day 5 and Tg infected mice at day 10 post-infection.*** 200 Hp larvae were given to mice 7 days prior to infection with 20 Tg tissue cysts. IL-4 (top) and IL-13 (bottom) gene expression was measured by quantitative RT-PCR in the small intestine (A), the Peyer's Patches (B), the mesenteric lymph nodes (C), the spleen (D) and the liver (E) at 5 (left) and 10 (right) days post Tg-infection. N= 2-4 mice per group per experiment, 2 independent experiments. Data was tested for normality (Anderson-Darling normality test). ANOVA or Kruskal-Wallis tests were performed on parametric/non-parametric pooled data, and when significant, Sidak's/Dunn's Multiple comparisons were performed on Hp vs. HpTg and Tg vs. HpTg; n.s. = non significant, * = $p<0.05$, ** = $p<0.01$ and ***= $p<0.001$.

Figure 5: ***IL-10 gene expression profiles in HpTg infected mice mirror those of Tg infected mice.*** 200 Hp larvae were given to mice 7 days prior to infection with 20 Tg tissue cysts. IL-10 gene expression was measured by quantitative RT-PCR in the small intestine (A), the Peyer's Patches (B), the mesenteric lymph nodes (C), the spleen (D) and the liver (E) at 5 (left) and 10 (right) days post -infection. N= 2-4 mice per group per experiment, 2 independent experiments. Data was tested for normality (Anderson-Darling normality test). ANOVA or Kruskal-Wallis tests were performed on parametric/non-parametric pooled data, and when significant, Sidak's/Dunn's Multiple comparisons were performed on Hp vs. HpTg and Tg vs. HpTg; n.s. = non significant, * = $p<0.05$, ** = $p<0.01$ and ***= $p<0.001$.

Figure 6: Compared to Tg infected mice, HpTg infected mice have a decrease in IFNγ-producing NK, CD8 T, NKT, γδ T and CD4 T cells in the MLN at d5 post Tg infection. 200 *H. polygyrus* larvae were given to mice 7 days prior to infection with 20 Me49 *T. gondii* tissue cysts. (A). The total number of viable cells was counted for the MLN at d5. MLN cell populations were assessed by flow cytometry. (B) The cell percentage (left) and total number (right) of NK (1st row), NKT (2nd row), yd T (3rd row), CD4 (4th row) and CD8 (5th row) cells. (C) The cell percentage (left) and total number (right) of IFN□-producing NK (1st row), NKT (2nd row), γδ T (3rd row), CD4 (4th row) and CD8 (5th row) cells. (C) The cell percentage (left) and total number (right) of GRZb-producing NK (1st row), NKT (2nd row), yd T (3rd row), CD4 (4th row) and CD8 (5th row) cells. N= 2-4 mice per group per experiment, 2 independent experiments. Data was tested for normality (Anderson-Darling test). ANOVA or Kriskal-Wallis tests were performed on parametric/non-parametric pooled data, and when significant, Sidak's/Dunn's Multiple

comparisons were performed on Hp vs. HpTg and Tg vs. HpTg; n.s. = non significant, * = $p<0.05$, ** = $p<0.01$, ***= $p<0.001$ and ****= $p<0.0001$.

Figure 7: At d5 post Tg infection in the PP, the HpTg infected mice have decreased proportions of IFNγ producing CD8 T cells compared to Tg infected mice. 200 *H. polygyrus* larvae were given to mice 7 days prior to infection with 20 Me49 *T. gondii* tissue cysts. PP cell populations were assessed by flow cytometry. (A) The proportion of NK (left), IFNγ-producing NK cells (middle) and GZB- producing NK cells (right). (B) The proportion of CD8 T (left), IFNγ-producing CD8 T cells (middle) and GZB- producing CD8 T cells (right). (C) The proportion of NKT (left), IFN-producing NKT cells (middle) and GZB-producing NKT cells (right). (D) The proportion of gd T cells (left), IFNγ-producing γδ T cells (middle) and GZB-producing γδ T cells (right). (E) The proportion of CD4 T cells (left), IFNγ-producing CD4 T cells (middle) and GZB-producing CD4 T cells (right). N= 2-4 mice per group per experiment, 2 independent experiments. Data was tested for normality (Anderson-Darling test). ANOVA or Kriskal-Wallis tests were performed on parametric/non-parametric pooled data, and when significant, Sidak's/Dunn's Multiple comparisons were performed on Hp vs. HpTg and Tg vs. HpTg; n.s. = non significant, * = $p<0.05$, ** = $p<0.01$, ***= $p<0.001$ and ****= $p<0.0001$.

SUPPLEMENTARY DATA

Supplementary Figure 1: ***The spleen pathology scale.*** (A). Follicle damage: All follicles are distinct and defined in shape (score of 1, top left). A majority of follicles are distinct and defined

in shape (score of 2, top middle). Approximately equal numbers of intact and damaged follicles. (score of 3, top right). The majority of follicles are damaged, with some defined follicles observed (score of 4, bottom left). All follicles are damaged (score of 5, bottom right). Scale 10um. (B) Marginal zone thickness: More than 50% of the follicles have a thick marginal zone (score of 1, left). More than 50% of the follicles have a thin marginal zone (score of 2, middle) More than 50% of the follicles do not have an observable marginal zone (score of 3, right). (C) Size of the light zone of the germinal centre: More than 50% of the follicles have a small germinal center (score of 1, left). More than 50% of the follicles have a large germinal center (score of 2, middle). More than 50% of the follicles have no observable germinal center (score of 3, right).

Supplementary Figure 2: ***The liver pathology scale.*** (A). Necrosis: absence (score of 1, left) and presence (score of 2, right) of necrosis. Scale 10um. (B) Infiltrate Size: All infiltrates observed are organized into small groups (score of 1, left), 75% of infiltrates observed are organized into small groups and 25% into large groups (score of 2, middle left), 50/50 split between small and large infiltrate groups (score of 3, middle right), 100% of infiltrates are organized into large groups (score of 4, right). (C). Proportion of infiltrates: very few infiltrate groups are observed (score of 1, top left), some groups of infiltrates are observed (score of 2, top middle), a medium number of infiltrates is observed (score of 3, top right), many infiltrate groups are observed and occupy the majority of the tissue (score of 4, bottom left), infiltrate groups are distinguishable, and occupy most of the tissue (score of 5, bottom middle), and Infiltrate groups are indistinguishable and occupy the entire tissue (score of 6, bottom right). (D) Perivascular

infiltrates: Very few infiltrating leukocytes can be observed in the vessels (score of 1, left). Infiltrating leukocytes are observed in small numbers leaving most of the vessels (score of 2, left middle). Most of the vessels are surrounded by infiltrating leukocytes (score of 3, right middle). All of the vessels are filled with infiltrating leukocytes (score of 4, right).

Supplementary Figure 3: ***The flow cytometry gating strategy.*** (A). FSC-A vs. FSC-H (left) and SSC-A vs. SSC-W (right) were used to exclude doublets. (B) Lymphocytes were identified using a viability stain (left), a CD45 stain (middle left) and the FSC-A vs. SSC-A parameters (middle right). CD3 was used to discriminate between the CD3- lymphocytes (NK cells) and the CD3+ lymphocytes (NKT, CD4 T, CD8 T and $\gamma\delta$ T cells). (C) NK1.1 identified NK cells (left). IFNg and GrzmB producers were detected using FMOs. (D) CD3+ cells were split into $\gamma\delta$ T cells, NK T cells and conventional T cells using FMOs (left and middle), conventional T cells were further defined as CD4+ and CD+ T cells (right). (E) IFNg and GrzmB producing $\gamma\delta$ T cells were detected using FMOs. (F) IFNg and GrzmB producing NK T cells were detected using FMOs. (G) IFNg and GrzmB producing CD8+ T cells were detected using FMOs. (H) (F) IFNg and GrzmB producing CD4+ T cells were detected using FMOs.

ACKNOWLEDGEMENTS

We would like to thank the University of Calgary LESARC Facility technicians, especially Dawn Martin for their continued support.

This works was funded through Dr. Finney's grants from the Canadian Foundation for Innovation and the Natural Sciences and Engineering Research Council of Canada (NSERC), as well as scholarships for Dr Anupama Ariyaratne (NSERC Create in Host Parasite Interactions), Namratha Badawadagi (University of Calgary Markin scholarship), Kayla Bailey (University of Calgary PURE Scholarship), Dr Joel Bowron (NSERC), Camila Gaio and Manfred Ritz (Mitacs Globalinks Scholarships,) and Dr Edina Szabo (UCalgary Eyes High Postdoctoral Scholarship).

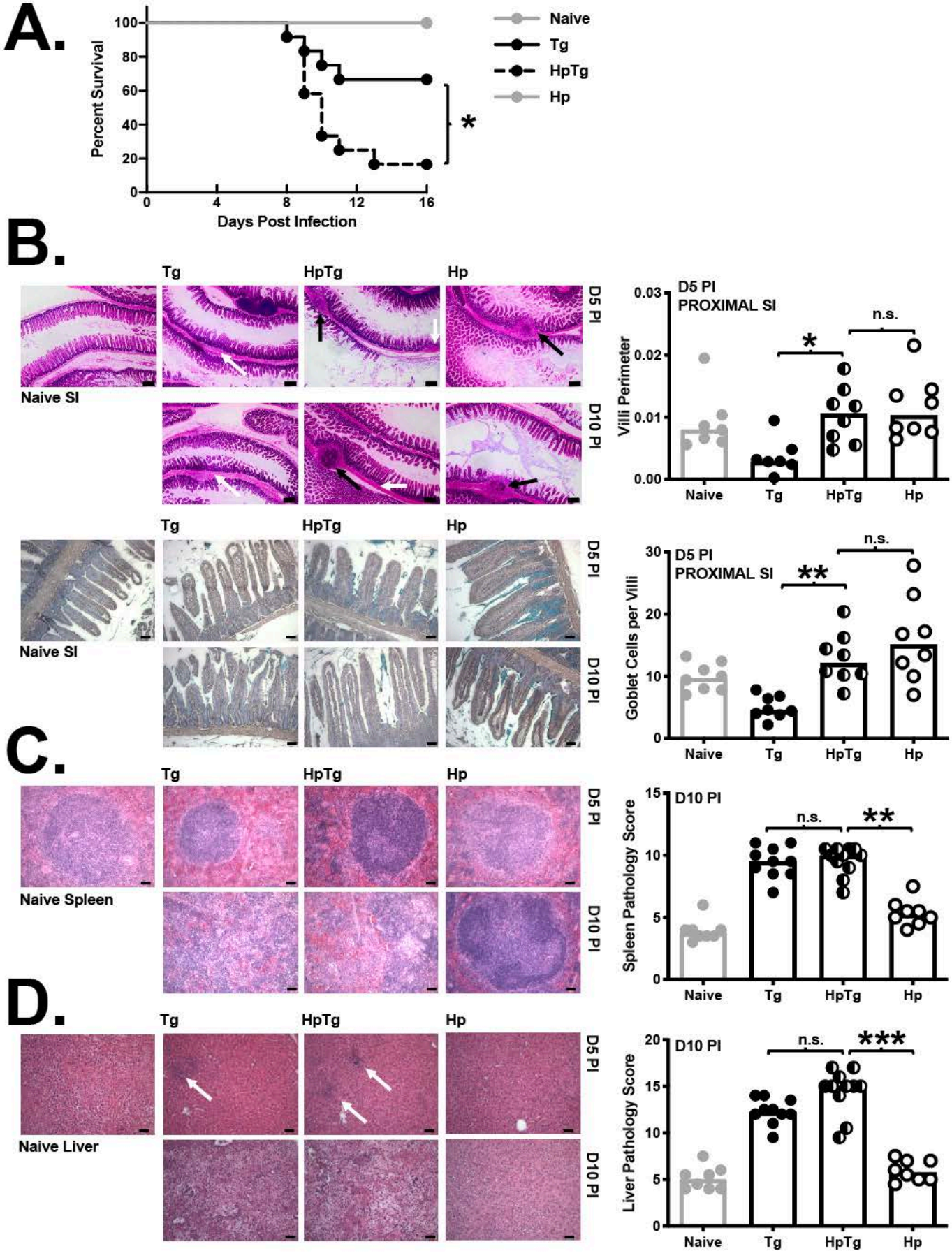
A.
Percent Survival
100
80
60
40
20
0
0
4
8
12
16
Days Post Infection
Naive
Tg
HpTg
Hp
*
B.
Tg
HpTg
Hp
D5 PI
D10 PI
Naive SI
D5 PI
PROXIMAL SI
Villi Perimeter
0.03
0.02
0.01
0.00
*
n.s.
Naive
Tg
HpTg
Hp
Tg
HpTg
Hp
D5 PI
D10 PI
Naive SI
D5 PI
PROXIMAL SI
Goblet Cells per Villi
30
20
10
0
**
n.s.
Naive
Tg
HpTg
Hp
C.
Tg
HpTg
Hp
D5 PI
D10 PI
Naive Spleen
D10 PI
Spleen Pathology Score
15
10
5
0
n.s.
**
Naive
Tg
HpTg
Hp
D.
Tg
HpTg
Hp
D5 PI
D10 PI
Naive Liver
D10 PI
Liver Pathology Score
20
15
10
5
0
n.s.
***
Naive
Tg
HpTg
Hp

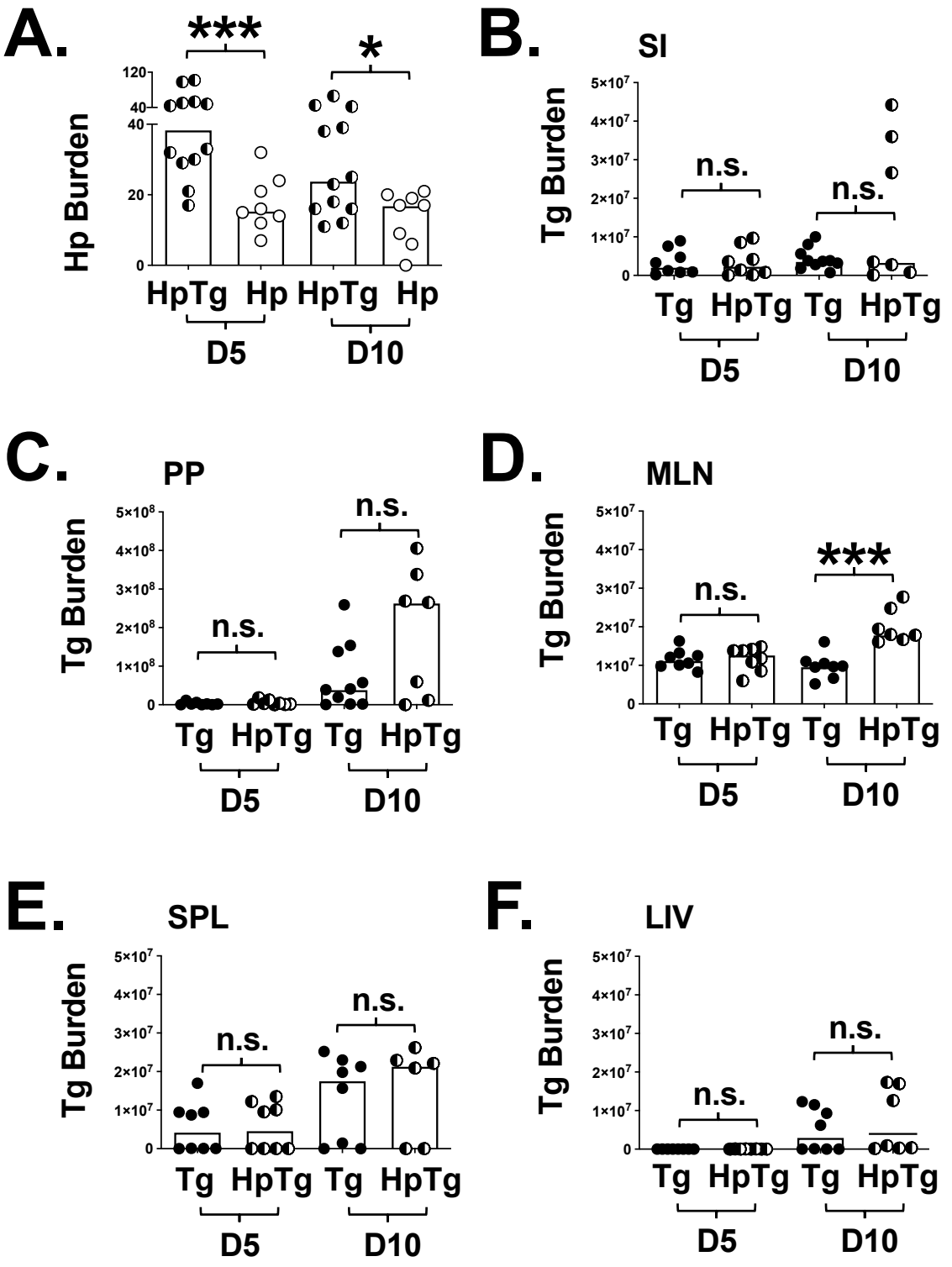
A.
***
*
Hp Burden
120
40
40
20
0
HpTg Hp HpTg Hp
D5
D10
B.
SI
Tg Burden
5×10^7
4×10^7
3×10^7
2×10^7
1×10^7
0
n.s.
n.s.
Tg HpTg Tg HpTg
D5
D10
C.
PP
Tg Burden
5×10^8
4×10^8
3×10^8
2×10^8
1×10^8
0
n.s.
n.s.
Tg HpTg Tg HpTg
D5
D10
D.
MLN
Tg Burden
5×10^7
4×10^7
3×10^7
2×10^7
1×10^7
0
n.s.
***
Tg HpTg Tg HpTg
D5
D10
E.
SPL
Tg Burden
5×10^7
4×10^7
3×10^7
2×10^7
1×10^7
0
n.s.
n.s.
Tg HpTg Tg HpTg
D5
D10
F.
LIV
Tg Burden
5×10^7
4×10^7
3×10^7
2×10^7
1×10^7
0
n.s.
n.s.
Tg HpTg Tg HpTg
D5
D10

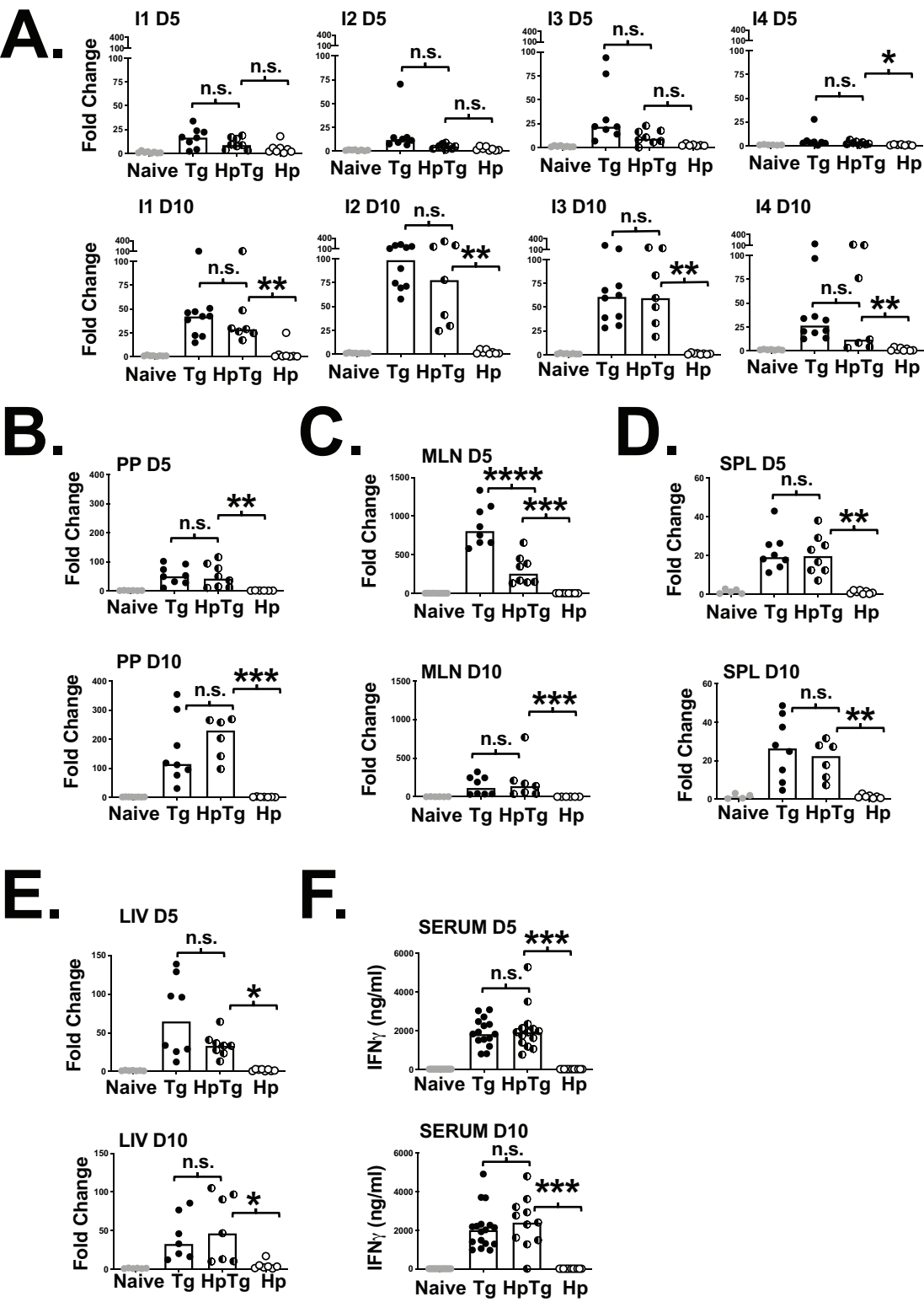
A.
I1 D5
I2 D5
I3 D5
I4 D5
I1 D10
I2 D10
I3 D10
I4 D10
Fold Change
Naive Tg HpTg Hp
n.s.
*
**
B.
PP D5
PP D10
C.
MLN D5
MLN D10
D.
SPL D5
SPL D10
E.
LIV D5
LIV D10
F.
SERUM D5
SERUM D10
IFNγ (ng/ml)
***
****

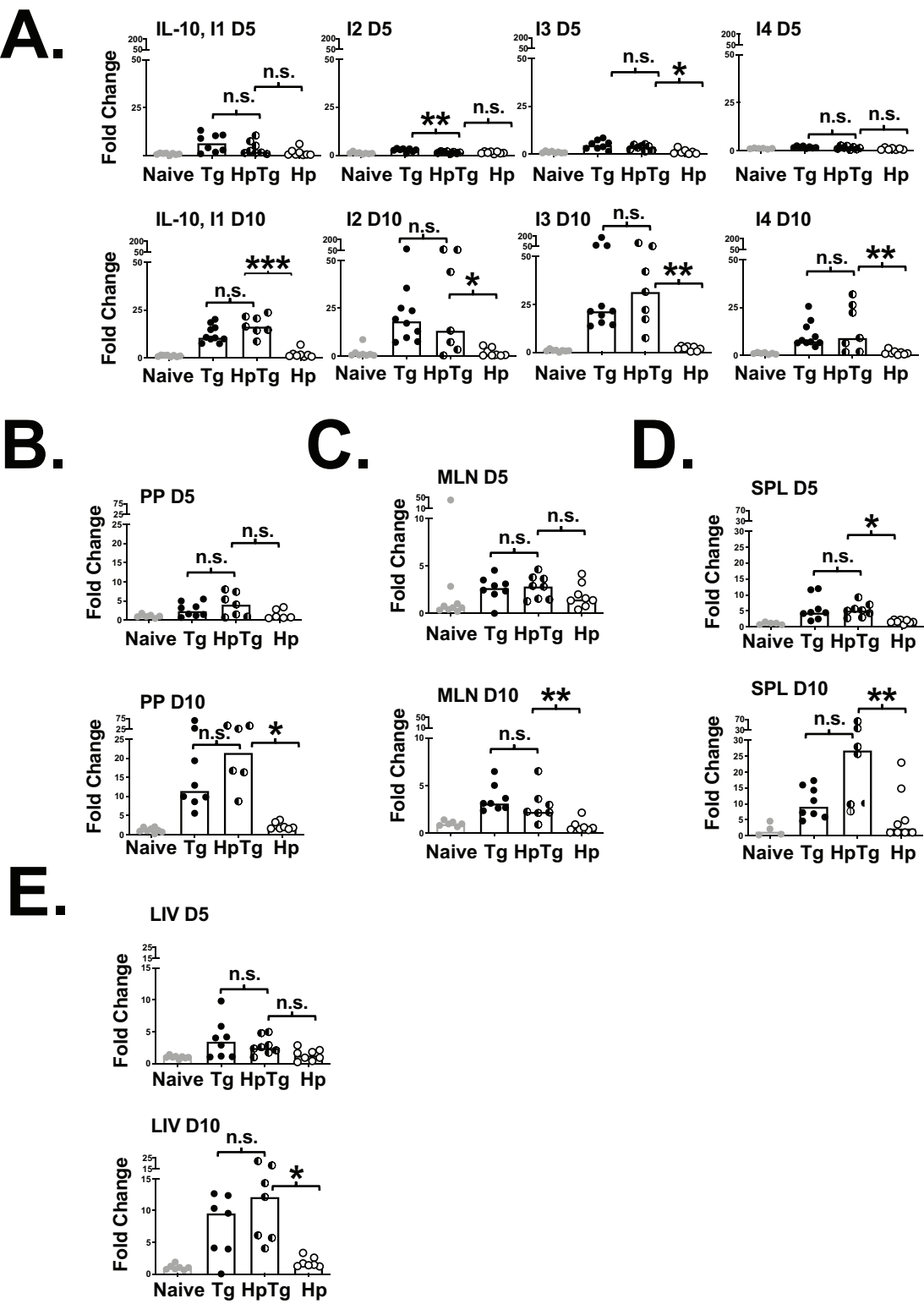
A.
IL-10, Il1 D5
Il2 D5
Il3 D5
Il4 D5
IL-10, Il1 D10
Il2 D10
Il3 D10
Il4 D10
Fold Change
Naive Tg HpTg Hp
n.s.
**
*
***
B.
PP D5
PP D10
C.
MLN D5
MLN D10
D.
SPL D5
SPL D10
E.
LIV D5
LIV D10

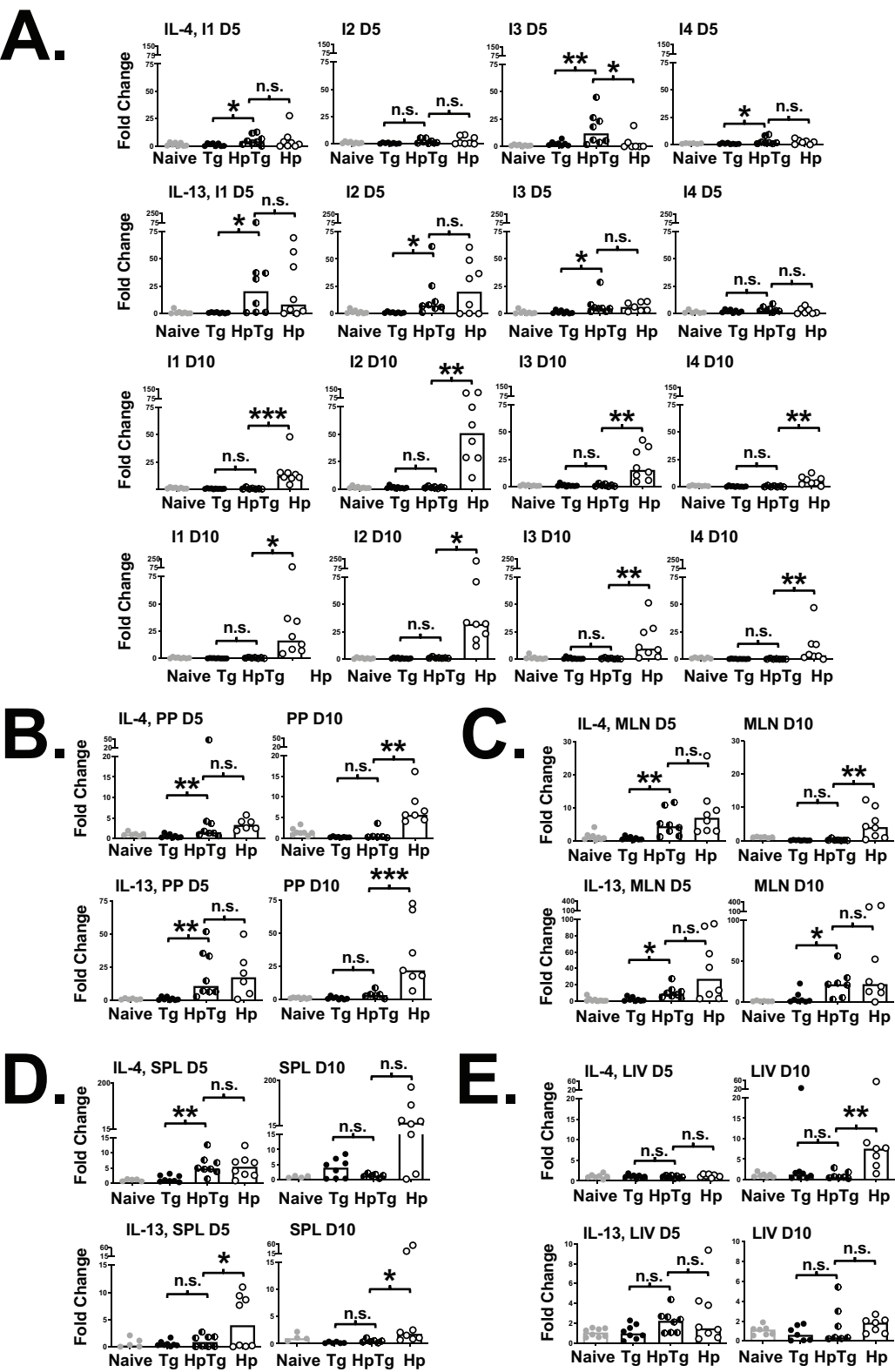
A.
IL-4, I1 D5
I2 D5
I3 D5
I4 D5
IL-13, I1 D5
I2 D5
I3 D5
I4 D5
I1 D10
I2 D10
I3 D10
I4 D10
I1 D10
I2 D10
I3 D10
I4 D10
Fold Change
Naive Tg HpTg Hp
n.s.
B.
IL-4, PP D5
PP D10
IL-13, PP D5
PP D10
C.
IL-4, MLN D5
MLN D10
IL-13, MLN D5
MLN D10
D.
IL-4, SPL D5
SPL D10
IL-13, SPL D5
SPL D10
E.
IL-4, LIV D5
LIV D10
IL-13, LIV D5
LIV D10

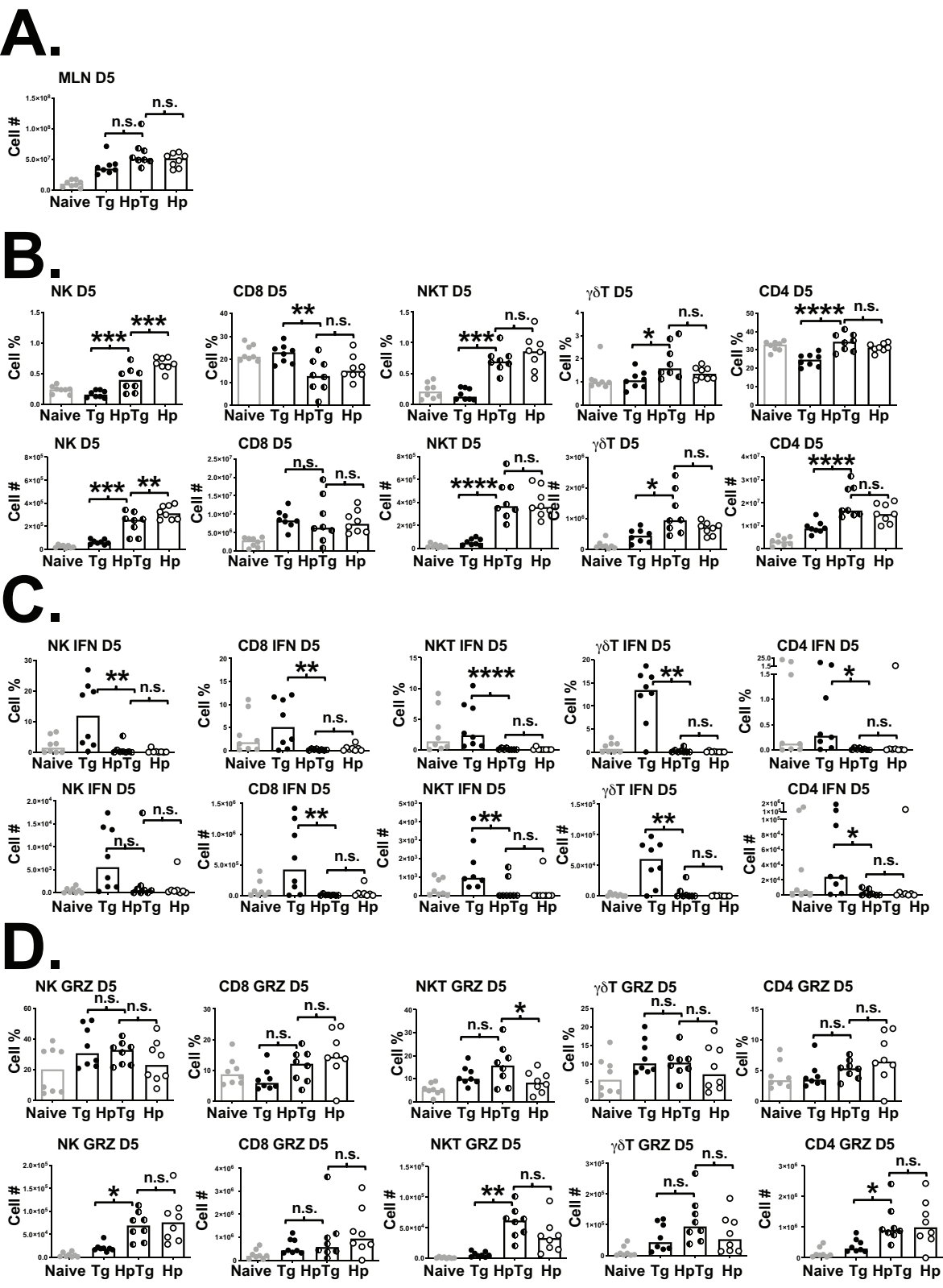
A.
MLN D5
Cell #
n.s.
n.s.
Naive Tg HpTg Hp
B.
NK D5
CD8 D5
NKT D5
γδT D5
CD4 D5
Cell %
Cell #
Naive Tg HpTg Hp
C.
NK IFN D5
CD8 IFN D5
NKT IFN D5
γδT IFN D5
CD4 IFN D5
D.
NK GRZ D5
CD8 GRZ D5
NKT GRZ D5
γδT GRZ D5
CD4 GRZ D5

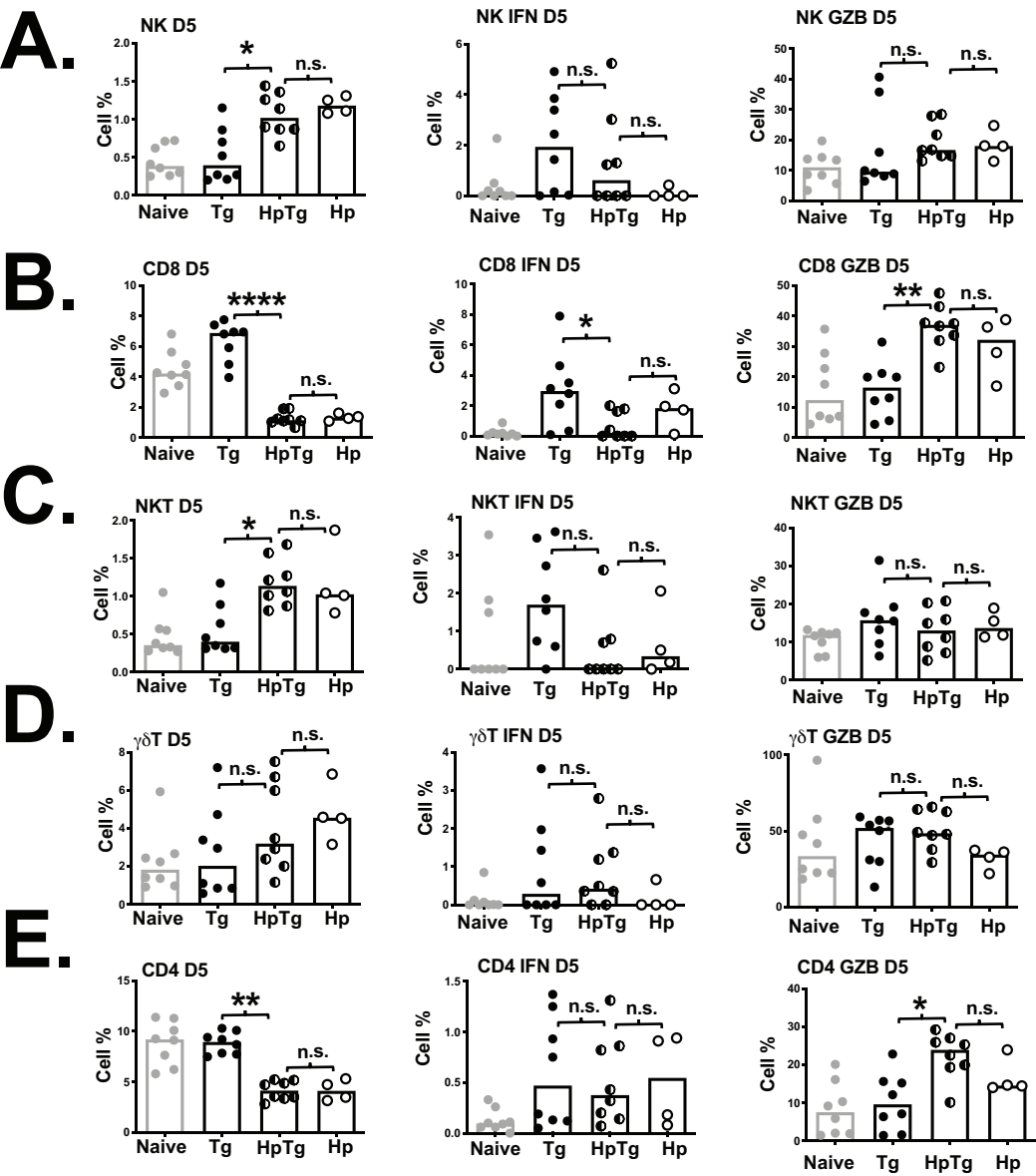
A.
NK D5
NK IFN D5
NK GZB D5
B.
CD8 D5
CD8 IFN D5
CD8 GZB D5
C.
NKT D5
NKT IFN D5
NKT GZB D5
D.
γδT D5
γδT IFN D5
γδT GZB D5
E.
CD4 D5
CD4 IFN D5
CD4 GZB D5
Cell %
Naive
Tg
HpTg
Hp
n.s.

A.

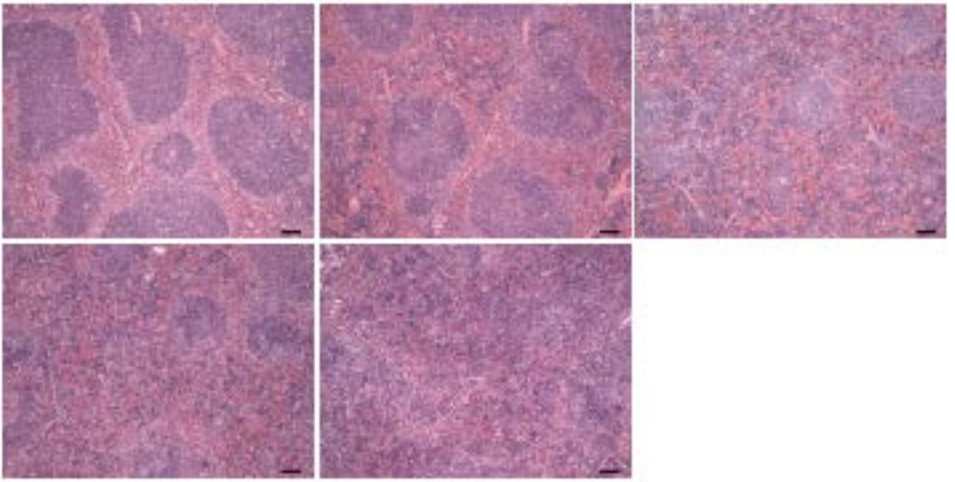

B.

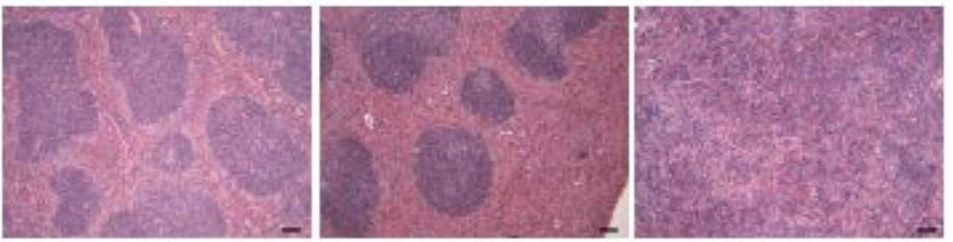

C.

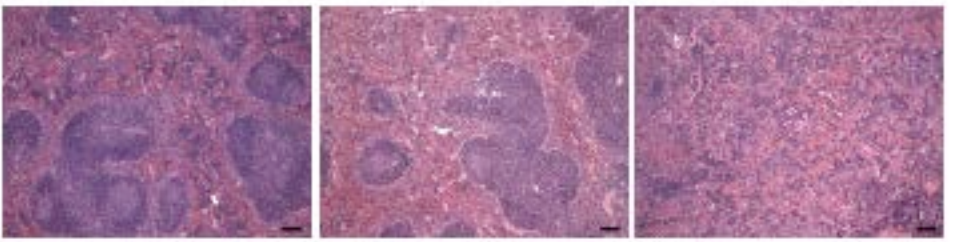

A.

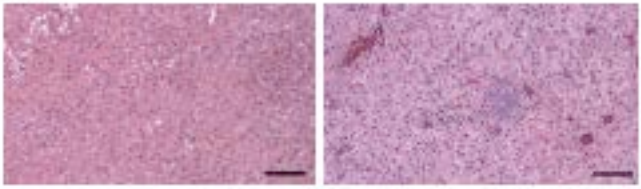

B.

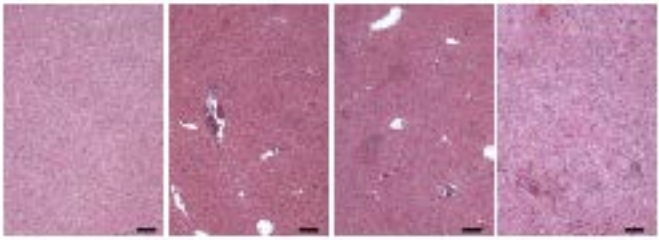

C.

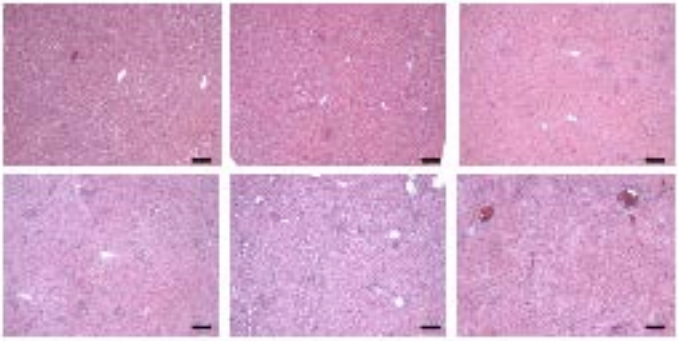

D.

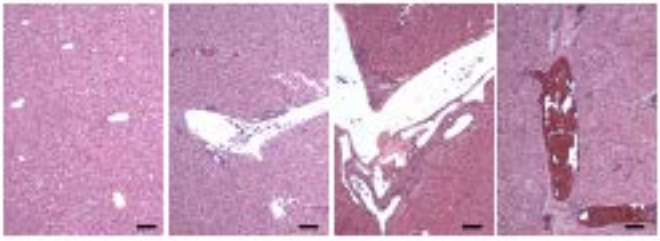

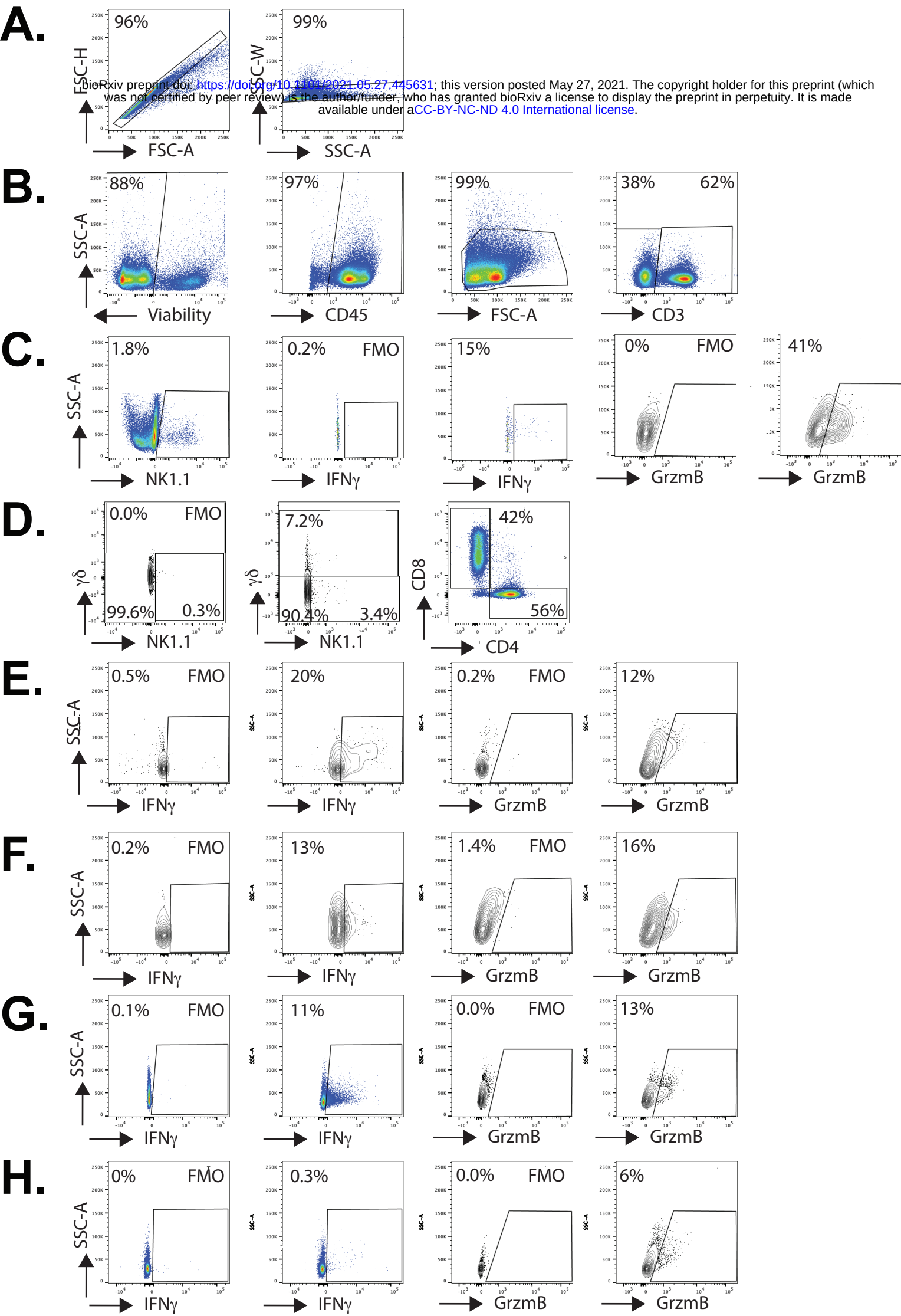

Group	Villi	Pathology	Distribution		Peyers Patches
			Proximal	Distal	
Naive	Tall and thin	Few and small infiltrates	Randomly across small intestine	Randomly across small intestine	Appear normal
Hp D5	Distorted around granulomas	Discontinuous & severe (granulomas)	Most granulomas	Similar to naïve tissue.	Appear normal
Hp D10	Distorted around granulomas	Discontinuous & severe (granulomas) and mild infiltrates	Most granuloma	Mild infiltrates found here.	Appear normal
Tg 5	Distorted around inflammation	Discontinuous & mild (infiltrates)	Little pathology	Most pathology	Appear normal
Tg 10	Distorted around inflammation	Increased frequency, severity and continuity.	Pathology	Pathology	Appear disorganised
HpTg 5	Distorted where pathology	Discontinuous mild/moderate inflammation (Tg) & granulomas (Hp)	Pathology (mostly granulomas)	Pathology (mostly infiltrates)	Appear normal
HpTg 10	Distorted where pathology	Severe & more continuous	Pathology	Pathology	Appear disorganised

Supplementary Table 1 Intestinal pathology of the different experimental groups. Results are based on observing H&E sections of whole small intestine swiss rolls on a dissecting microscope. Data are from 2 pooled experiments for each time point where n = 2-4 animals per group.

Parameter	Definition	Score
Follicle Shape	All follicles are distinct and defined in shape.	1
	The majority of follicles are distinct in shape but some are damaged (75% vs. 25%).	2
	Approximately half of the follicles are damaged	3
	The majority of follicles are damaged, but some defined follicles are observed. (75% vs. 25%).	4
	All follicles are damaged, to the point where they are indistinguishable from the rest of the tissue.	5
Marginal Zone	>50% of follicles have a thick marginal zone.	1
	>50 % of follicles have a thin marginal zone.	2
	>50 % of follicles have no observable marginal zone.	3
Germinal Center (Light Zone)	>50% of follicles have a small germinal center.	1
	>50% of follicles have a large germinal center.	2
	>50% of follicles have no observable germinal center.	3

Supplementary Table 2 Spleen Pathology Scale. The total score for each animal was calculated by adding the score for the pathology associated with the follicle shape, the marginal zone and the germinal centre

Parameter	Definition	Score
Necrosis	No necrosis observed	1
	Necrosis observed	2
Infiltrate Size	All infiltrates observed are organized into small groups	1
	75% of infiltrates observed are organized into small groups and 25% into large groups	2
	50/50 split between small and large infiltrate groups	3
	100% of infiltrates are organized into large groups	4
Proportion of Infiltrates	Very few infiltrate groups are observed (e.g. 1-2)	1
	Some groups of infiltrates are observed.	2
	A medium number of infiltrates is observed.	**3**
	Many infiltrate groups are observed. They occupy the majority of the tissue.	4
	Infiltrate groups are distinguishable, and occupy most of the tissue.	5
	Infiltrate groups are indistinguishable and occupy the entire tissue.	6
Perivascular Infiltrates	Very few infiltrating leukocytes can be observed in the vessels.	1
	Infiltrating leukocytes are observed in small numbers leaving most of the vessels.	2
	Most of the vessels are surrounded by infiltrating leukocytes.	3
	All of the vessels are filled with infiltrating leukocytes.	4

Supplementary Table 3 Liver Pathology Scale. The total score for each animal was calculated by adding the score for the pathology associated with necrosis, the infiltrate size, the proportion of infiltrates and the nature of the perivascular infiltrates.